Chem Soc Rev

REVIEW ARTICLE

View Article Online
View Journal | View Issue

Check for updates

Cite this: *Chem. Soc. Rev.*, 2018, **47**, 4642

The geometry of periodic knots, polycatenanes and weaving from a chemical perspective: a library for reticular chemistry

Yuzhong Liu, [a] Michael O'Keeffe,*[b] Michael M. J. Treacy [c] and Omar M. Yaghi *[ad]

Received 30th September 2017

DOI: 10.1039/c7cs00695k

rsc.li/chem-soc-rev

The geometry of simple knots and catenanes is described using the concept of linear line segments (sticks) joined at corners. This is extended to include woven linear threads as members of the extended family of knots. The concept of transitivity that can be used as a measure of regularity is explained. Then a review is given of the simplest, most 'regular' 2- and 3-periodic patterns of polycatenanes and weavings. Occurrences in crystal structures are noted but most structures are believed to be new and ripe targets for designed synthesis.

Published on 04 May 2018. Downloaded by University of California - Berkeley on 6/22/2018 6:56:28 PM.

1. Introduction

1.1 Knots, catenanes and weaving

If a knot is tied in a length of string and then the ends of the string are joined, one will have a knotted loop. This is what mathematicians consider as a knot. If a drawing is made of the knot it will be found that, at points, pieces of string cross. The minimal number of crossings in such a drawing is the crossing number of the knot. To make a knot in a single loop, one needs at least 3 crossings (*i.e.* crossing number = 3, Fig. 1).

Suppose now two loops are linked together so they cannot be separated without breaking the string – this also is a knot. The simplest such link (a *Hopf link*) has a crossing number of 2.

Knots are given a symbol n_k^m indicating that m loops form a knot with n crossings. k is an arbitrary serial number to distinguish knots with the same values of n and m. A comprehensive listing of knots can be found at the *Knot Atlas.*[1] A good introduction to knot theory for the non-mathematicians is the book by Adams.[2]

In chemistry, linked molecular loops (rings) are known as catenanes and multiple linked rings are polycatenanes.[3,4] Molecular knots and catenanes have been studied extensively for 50 years and are the subject of excellent reviews.[5–8]

[a] *Department of Chemistry, University of California-Berkeley, Materials Sciences Division, Lawrence Berkeley National Laboratory, Kavli Energy NanoSciences Institute, Berkeley, California 94720, USA. E-mail: yaghi@berkeley.edu*
[b] *School of Molecular Sciences, Arizona State University, Tempe, AZ 85287, USA. E-mail: mokeeffe@asu.edu*
[c] *Department of Physics, Arizona State University, Tempe, AZ 85287, USA*
[d] *King Abdulaziz City for Science and Technology, Riyadh 11442, Saudi Arabia*

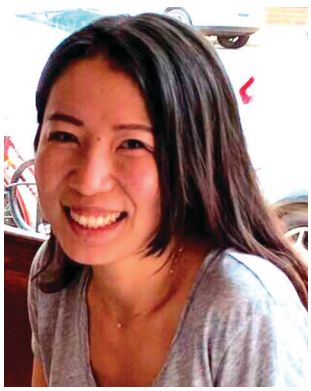

Yuzhong Liu

Yuzhong Liu grew up in Hangzhou, China and went on to pursue her BSc degree in Chemistry at University of Michigan, Ann Arbor where she discovered snow and her passion for chemistry. After graduation, she took a gap year and developed chemical tools for neurodegenerative diseases such as Alzheimer's Disease under the guidance of Professor Mi Hee Lim. In 2013, Yuzhong started graduate school at UC Berkeley and joined Professor Omar Yaghi's group. Her research interest now focuses on the design and synthesis of crystalline woven covalent organic frameworks.

Michael O'Keeffe

Michael O'Keeffe was born in Bury St. Edmunds, England in 1934, He attended Bristol University. Since 1963 he has been at Arizona State University where he is currently Regents' Professor Emeritus. His research interests have ranged widely over solid state chemistry. In recent years, he has been particularly interested in the geometry of periodic structures such as nets, tilings, and weavings, and in its relevance to the design and synthesis of crystalline materials.

This journal is © The Royal Society of Chemistry 2018

Published on 04 May 2018. Downloaded by University of California - Berkeley on 6/22/2018 6:56:28 PM.

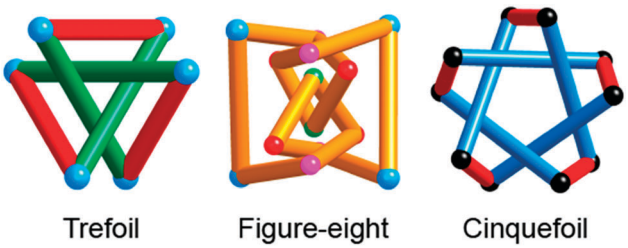

Fig. 1 The simplest knots shown as sticks and corners. In the trefoil and cinquefoil knots, symmetry-related sticks have the same color.

In this article, we present an approach to this subject with an emphasis on periodic structures from the point of view of reticular chemistry.[9] In reticular chemistry atoms, or molecular groups of atoms (secondary building units, SBUs), are joined by links into symmetrical frameworks notably in materials such as metal–organic frameworks (MOFs)[10] and covalent organic frameworks (COFs).[11] The geometry is abstracted as nodes joined by straight links. In application to knots and related structures the straight links are called sticks. They meet in pairs at two-coordinated vertices (we term these corners). The loops of knots now become (generally non-planar) polygons. In the jargon, such embeddings of knots are referred to as piecewise linear. This article is concerned with piecewise linear descriptions of polycatenanes and weavings.

In modern mathematics of, for example, periodic polyhedra (Grünbaum–Dress polyhedra),[12] faces (rings) are allowed to become infinite and take shapes such as zigzags and helices with linear segments. Accordingly, we consider entanglement (weaving) of threads as part of the same structure family as knots and catenanes. In particular, we consider threads as also made up of corners and sticks.

For many structures, we give a three-letter (lower case, bold) identifying symbol. In some cases, we use the symbols **abc-w** and **abc-y** for respectively a weaving or a polycatenane derived from a 3-periodic net **abc**, which can be found in the RCSR database.[13]

1.2 Transitivity, the minimal transitivity principle and regular structures

In the theory of graphs (nets) and tilings, vertices related by the intrinsic symmetry are said to be the same kind. If there are p kinds of vertex the graph is vertex p-transitive. For a net characterizing a crystal structure the transitivity $p\ q$ indicates that there are p kinds of vertex and q kinds of edge.

Of the more than six million distinct polyhedra with 12 vertices only the five vertex 1-transitive (often abbreviated to 'vertex transitive' when $p = 1$) are of special interest in chemistry. Similarly, of the essentially infinite number of periodic graphs (nets) the principle of minimal transitivity states that the net formed by linking SBUs is likely to have the minimal transitivity consistent with the starting materials.[14]

In tilings of the sphere (polyhedra) or 2-dimensional tilings, the transitivity $p\ q\ r$ indicates that there are p kinds of vertex, q kinds of edge and r kinds of face. The five regular polyhedra and three regular plane tilings are those with transitivity 1 1 1.[15] They are of special importance to structural chemistry.

For crystal nets, we have the algorithms of Systre to determine the symmetry and transitivity.[16] However for knots and weavings, we must determine the symmetry by inspection then construct a model with sticks and corners and finally determine the transitivity *pqr* which now indicates the numbers of kinds of, respectively, corners, sticks and rings or threads. Note that as different rings and threads do not share corners or sticks p and q must be $\geq r$. Structures with transitivity 1 1 1 we term regular. We find that 3-periodic catenanes and weavings are

Michael M. J. Treacy

Michael Treacy was born in Ireland and raised in Portsmouth, UK. He graduated from Cambridge, UK, with an MA in physics and a PhD in transmission electron microscopy of catalysts. He joined Exxon in New Jersey, USA, to work on the structural characterization of zeolites. He later moved to the NEC Research Institute in Princeton, where he worked on TEM structural characterization of nanotubes, ferroelectrics and amorphous materials, and continued his interests in zeolites. In 2003, he joined the physics department at Arizona State University. His current research interests are in the structural topologies of amorphous materials and framework materials, including zeolites. He was chair of the Structure Commission of the International Zeolite Association for 15 years.

Omar M. Yaghi

Omar M. Yaghi received his PhD from the University of Illinois-Urbana, and studied as an NSF Postdoctoral Fellow at Harvard University. He is currently the James and Neeltje Tretter Chair Professor of Chemistry at UC Berkeley and a Senior Faculty Scientist at Lawrence Berkeley National Laboratory. He is also the Founding Director of the Berkeley Global Science Institute as well as the Co-Director of the Kavli Energy NanoScience Institute and the California Research Alliance by BASF. He is interested in the science of building chemical structures from organic and inorganic molecular building blocks (Reticular Chemistry) to make extended porous structures, such as MOFs, COFs, and ZIFs.

Published on 04 May 2018. Downloaded by University of California - Berkeley on 6/22/2018 6:56:28 PM.

particularly rich in regular structures, which should be prime targets for future synthesis.

1.3 Symmetry and symmetry groups

All of the structures we describe in detail are 3-dimensional. The 3-periodic structures have symmetry that is one of the 230 space groups. We assume the reader has some familiarity with these. The 2-periodic structures will have one of the 80 layer group symmetries.[17] It is one of the advantages of the Hermann–Mauguin system of symbols for symmetry groups that layer group symbols are interpreted exactly as space group symbols. The lattice is 2-dimensional and always defines the **ab** plane so there are no translational components of symmetry operations along **c**. Layer group symbols are distinguishable from space group symbols as the lattice symbol is always lower case (*p* or *c*). For 2-periodic weavings and polycatenanes, there is the further restriction that there cannot be a mirror normal to **c**. Remarkably, we have not found the symmetry of weavings given anywhere in the literature. A mathematical account of weaving simply states that the symmetry must be one of the seventeen 2-dimensional 'wallpaper' groups, but no symmetries were given.[18]

We briefly mention 1-periodic structure such as chains and braids. They have rod group symmetries. In one dimension, there is no crystallographic restriction of the order of rotations, but our examples have crystallographic symmetries recognizable as the lattice symbol is *p* for the 1-periodic lattice.

1.4 Related topics

Here we briefly mention some related topics that we do not discuss further in this article. These systems are not entirely based on weaving of threads and rings. They have been fully discussed elsewhere. We note that they are not directly concerned with the topic of periodic structures composed of solely corners and sticks – catenanes and weavings.

Interpenetrating nets. When periodic nets interpenetrate, rings on component nets become catenated. An early review described many compounds, particularly MOFs with structures based on interpenetrating nets.[19] Other detailed reviews of similar materials have ensued.[20–23] Several papers on the geometry of interpenetrating nets have also appeared. The introduction of the *Hopf ring net* (HRN) greatly aids in the characterization of interpenetration.[20] A comprehensive account of symmetrical embeddings and properties of interpenetrations has been given.[24] In that paper it was remarked that one of the first crystal structures (that of cuprite, reported over 100 years ago) was based on interpenetrating **dia** (diamond) nets and so was the first chemical structure observed to have catenated rings. In that paper, it was also remarked that in one reported crystal structure each ring was catenated to 634 others – far beyond the dreams of molecular chemists. A related paper[25] discussed the optimum embeddings of such nets from a group-theoretical viewpoint.

Rotaxanes. Many fascinating rotaxanes have been reported.[26–29] A simple rotaxane is not a knot. In periodic polyrotaxanes the components are interlocked but the formal description of the structures would require nodes of coordination number greater than two as well as corners and sticks. These structures have been reviewed recently.[19,30] A periodic MOF structure with macrocycles interlocked on links was reported[31,32] and a number of similar structures more recently[33–35] but these likewise do not fall in the scope of the present article.

DNA origami. The construction of geometric shapes from DNA strands, generally known as origami is sometimes referred to as weaving. However, it does not fit into the subject as discussed here and we simply refer the reader to recent comprehensive reviews.[36–38]

2. 0- and 1-periodic structures

2.1 Some simple knots

Knots are 3-dimensional and their symmetries are one of the point symmetry groups of Euclidean space. Fig. 1 shows the three simplest single-loop knots with respectively crossing numbers 3, 4, and 5. These are the structures of almost all reported molecular knots,[39–41] although a molecular knot with 8 crossings has recently been reported.[42]

Knots can always be formed from straight sticks and the stick number is the minimal number of sticks required. Minimal stick configurations generally have less than maximum symmetry. Here, we are interested in the maximum symmetry configurations and so our structures generally require more edges.

The trefoil knot, symmetry 32 (D_3) has transitivity 1 2 1 and can be formed from 6 sticks, so the stick number is 6. The cinquefoil knot, symmetry 52 (D_5), also has transitivity 1 2 1. In the symmetric conformation illustrated there are 10 sticks, but note that the stick number for this knot is 8. The figure-eight knot with crossing number 4 has only symmetry 222 (D_2) and transitivity 4 4 1 making it a much more challenging target for designed synthesis.[43]

2.2 Linked pairs of rings

The simplest pair of linked rings, the classical catenane, has crossing number 2 and is generally known as the *Hopf link*. It is shown in two ways in Fig. 2 to emphasize that the link cannot always be associated with just two corners. In the most symmetrical conformation (shown) the symmetry is $\bar{4}2m$ (D_{2d}) and the transitivity 2 2 1. For non-concentric linked rings, we can identify a *link point* as the barycenter (average of all corner vertices) of the two rings. An important step in synthetic chemistry was the introduction of using a metal template at the link point to facilitate the formation of catenanes.[44–48]

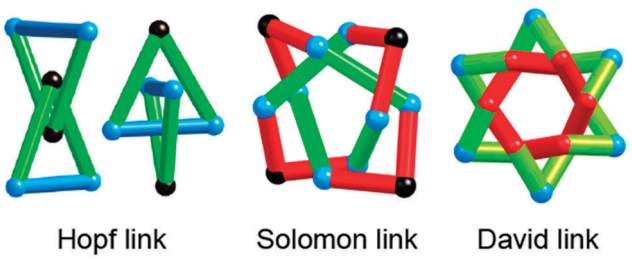

Fig. 2 The simplest links of pairs of rings. Sticks and corners of the same color are related by symmetry.

 This journal is © The Royal Society of Chemistry 2018

Published on 04 May 2018. Downloaded by University of California - Berkeley on 6/22/2018 6:56:28 PM.

Also shown are the double link (4 crossings) known as the *Solomon link* and the triple link. The latter has 12 edges, but in its most symmetrical form, it has 18 edges (Fig. 2) and has the shape of the star of David, so we call it the *David link*. Both these knots have transitivity 2 2 1.

2.3 Polycatenanes

Polycatenanes have more than two linked rings. There are two ways to link three rings so that each is linked to the other two (Fig. 3). There are six crossings and the knot symbols are 6_1^3 and 6_3^3. We meet 6_2^3, in which no pair of rings is linked, in the next section. The illustration of 6_1^3 (top right in the figure) clearly shows the six crossings and the symmetry 32 (D_3). Flipping one link (from over-under to under-over) converts 6_1^3 to 6_3^3 (top left in the figure) apparently destroying the symmetry. But surprisingly 6_3^3 also has an embedding with symmetry 32 as shown. We also show a piecewise linear embedding of 6_3^3 made with three triangles, again with symmetry 32 and transitivity 2 2 1. In that embedding three corners are now about a central symmetry point in a conformation we refer to in our descriptions of 3-periodic weavings as a triple crossing. Directed syntheses of a 6_3^3 [3]catenane have recently been reported.[49,50]

Also shown in the figure is the simplest form of a linear chain. This has symmetry $p4_2/mmc$ and transitivity 1 2 1. A chemical analogue has been reported recently.[51]

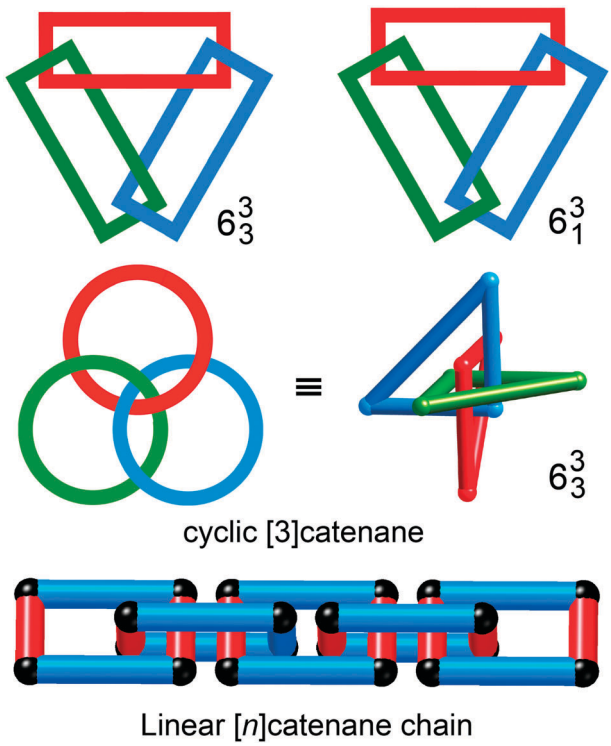

Fig. 3 Simple polycatenanes with Hopf links. Top: A cyclic [3]catenanes showing on left 6_3^3 and on the right 6_1^3. Below that are shown alternative embeddings of 6_3^3 with 32 (D_3) symmetry. The linear chain is an infinite catenane. In the embedding shown there is one kind of corner and two kinds of stick (red and blue).

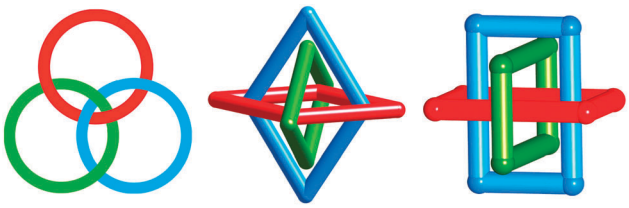

Fig. 4 Left: Borromean rings (knot 6_2^3) as circular loops. Center (transitivity 2 1 1) and right (transitivity 1 2 1) with cubic symmetry. Note that no two rings are linked. In the drawing on the right the corners are at the vertices of a regular icosahedron.

Later we show four rings with each linked to the other three. This has transitivity 1 1 1 and we believe it to be the simplest regular knot (transitivity 1 1 1).

2.4 Borromean rings

The famous Borromean rings are another way of linking 3 rings, again with six crossings, knot symbol 6_2^3. Fig. 4 shows the structure as interwoven circles. It can be seen that it may be derived from 6_3^3 (Fig. 5) by reversing the three outer crossings. In a maximum-symmetry embedding the structure is cubic, symmetry $m\bar{3}$ (T_h). Two embeddings as sticks in that symmetry are shown in Fig. 4: with one kind of corner, transitivity 1 2 1, and with one kind of stick, transitivity 2 1 1. This knot has what we term the Borromean property: although the rings are linked in the sense that no ring can be separated from the others without breaking sticks (links), no two rings are linked. Molecular Borromean rings have been achieved by directed assembly of eighteen components.[52]

2.5 Brunnian knots and braids

A Brunnian knot is composed of multiple rings and has the property that if one ring is removed the remaining rings are not linked. The Borromean rings are the simplest such Brunnian knot. Fig. 5 shows the first two of a series of Brunnian knots with three loops and a multiple of six crossings.

If the number of crossings is increased to infinity, the structure is that of a three-strand braid. The braid is intrinsically a rather simple structure, symmetry $p2/c$. As made with flexible strings (or hair) the configuration is as shown in the top illustration with transitivity 2 2 1. Braids are well known in materials like MOFs.[53] It is interesting that some of these have a less-curved embedding, also shown in the figure, that has the same symmetry but transitivity 1 2 1. The adoption and recognition of this structure emphasizes the utility of the stick-and-corner description of molecular structures.

A characteristic of three-component Brunnian structures, say green, red, blue, is that the crossings are such that green is over red, red over blue and blue over green (Fig. 5).

Also shown in the figure is a Brunnian chain of what are known as 'rubber band' links. Pairs of loops are not linked topologically and can be separated if sticks are allowed to bend. But the whole chain is linked. The symmetry is $p\bar{4}m2$ and the transitivity is 1 2 1.

Published on 04 May 2018. Downloaded by University of California - Berkeley on 6/22/2018 6:56:28 PM.

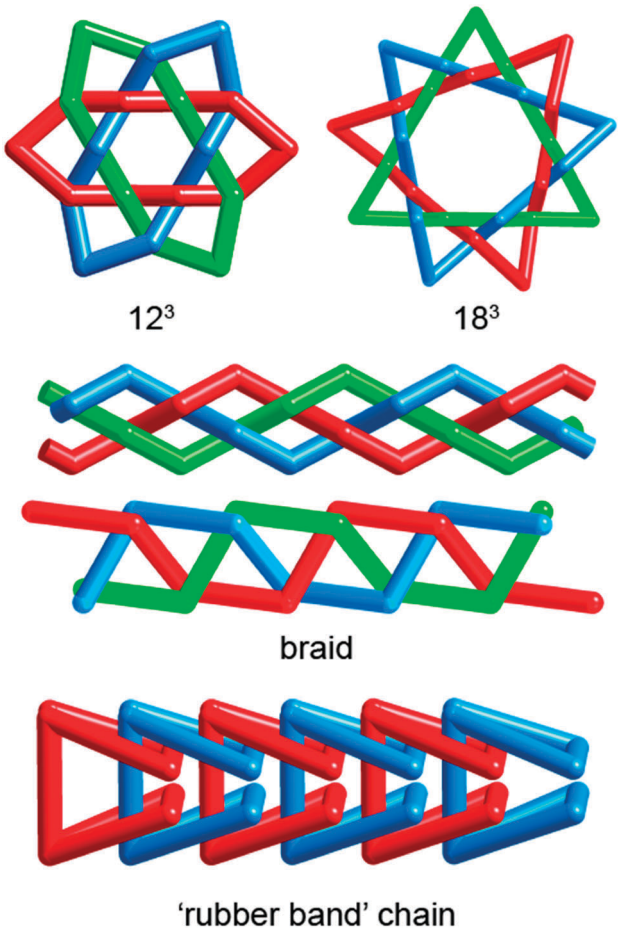

Fig. 5 Examples of Brunnian knots. The top two have three finite rings and removing one ring leaves the other two unlinked. The braid is the corresponding structure with infinite rings (threads). In the upper embedding there are two kinds of corner and one kind of stick (transitivity 2 1 1). In the lower, one kind of corner and two kinds of stick (transitivity 1 2 1). Note that in each case red is above blue, blue above green and green above red. The rubber band chain also has the Brunnian property. In a finite chain, rings at the end can be removed by bending, but not by breaking, the sticks.

2.6 Regular polycatenanes

We identify seven regular finite polycatenanes with transitivity 1 1 1 (Fig. 6). We have not found them formally described elsewhere, or realized as molecules, although some are familiar to model builders. We can confidently predict molecules based on these structures will be found in future. They can be considered as regular weavings on the sphere – on the sphere a thread becomes a ring – emphasizing again that polycatenanes and woven fabrics are part of the same structure family. Also shown in the figure (bottom right) is a well-known regular figure, symmetry 532 (*I*), composed of five catenated tetrahedra with vertices forming a regular rhombic dodecahedron. We know of no other finite regular figure formed from catenated polyhedra – we identify infinite periodic structures later.

The simplest regular polycatenane (knot) 12^4 is composed of four equilateral triangles, each linked to the other three, and has symmetry 432 (*O*). The vertices are at the positions of those

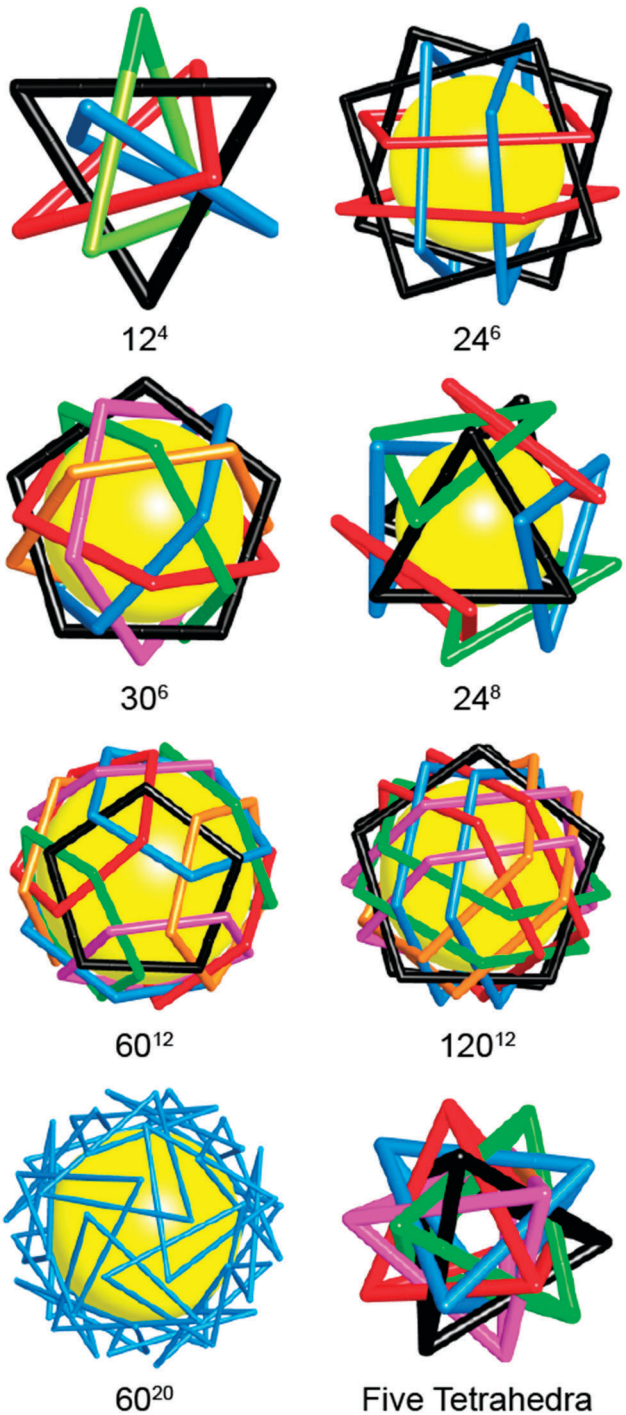

Fig. 6 Some regular polycatenanes and a regular linkage of five tetrahedra. For the polycatenanes p^q indicates p crossings and q rings (loops).

of a regular cuboctahedron (3.4.3.4). The ring link points are at the vertices of a regular tetrahedron.

The polycatenane 24^6, symmetry 432 (*O*), is made of six squares, each linked to four others. The corners form an Archimedean snub cube ($3^4.4$) and the link points form a cuboctahedron (3.4.3.4). The polycatenane 30^6, symmetry 532 (*I*), is formed from six concentric pentagons, each linked to the other five. The corners are at the vertices of an Archimedean

 This journal is © The Royal Society of Chemistry 2018

Published on 04 May 2018. Downloaded by University of California - Berkeley on 6/22/2018 6:56:28 PM.

icosidodecahedron (3.5.3.5). This structure is known as Makalu to origami enthusiasts.

The polycatenane 24^8 is formed from eight triangles, each linked to three others. The corners are at the vertices of a snub cube and the link points form a cuboctahedron (as in 24^6 above). The polycatenane 60^{12}, symmetry 532 (*I*), is formed from 12 pentagons, each linked to five others. The corners are at the vertices of an Archimedean snub dodecahedron ($3^4.5$). The polycatenane 120^{12}, symmetry 532 (*I*), is formed again from 12 pentagons, each now linked to ten others. The corners are again at the vertices of a snub dodecahedron. The polycatenane 60^{20}, symmetry 532 (*I*), is formed from 20 triangles each linked to three others. The corners are again at the vertices of a snub dodecahedron.

3. 2-Periodic structures

3.1 The lattice plane

In 2-periodic structures there will be an underlying lattice either primitive, symbol *p* or centered rectangular, symbol *c*. The lattice vectors are always **a** and **b**. They define a plane, the lattice plane of the structure.

3.2 Biaxial weaving

The weaving of threads into fabrics is one of the oldest human crafts and 2-periodic weaving patterns are found, for example, in MOFs. The classical (warp and woof) weavings are of threads in two directions at right angles (biaxial). The literature on ornamental weaving is vast, but of little relevance to our purpose, which is to identify structures of minimal transitivity.

We restrict ourselves to structures that have one kind of thread which have been termed isonemal.[18] Such threads are characterized by a sequence of integers (*p*,*q*,...) which states that at every crossing for a thread there are *p* over, followed by *q* under, followed by ... We just consider (*p*,*q*). With the exception of (2,2), for an isonemal weaving successive parallel rows must be displaced by one crossing. Such weaves are known as twills.

Weaving patterns are often illustrated by designs that show the weaving patterns by sequences of black and white squares for under and over crossings. Fig. 7 shows the design for a (3,2) twill. Note that the sequence of black and white is the same for every horizontal and vertical row as it must be for an isonemal weaving. If $p \neq q$ the fabric is not balanced – the two sides are not the same.

The first, and perhaps obvious, result is that there is just one regular biaxial weaving with transitivity 1 1 1 (Fig. 8). This is generally known as plain weave but also known as box weave, *calico*, *tabby*, *taffeta*, *etc.* We call attention to the symmetry *p*4/*nbm* that indicates the presence of all possible glides (*a*, *b*, *n*) in the layer lattice plane. It is the presence of such glides that adds to the attractiveness of weaving patterns. Fig. 8 also shows isonemal weavings (*p*,*q*) for $p \leq q \leq 3$. Clearly (*p*,*q*) is the same as (*q*,*p*) but viewed from the other side. Data for these structures are in Table 1.

The shape of the threads themselves is relevant to the design of crystals (Fig. 9). (1,1) gives a zigzag with transitivity (corners, sticks) = 1 1. (*p*,*p*) gives a 'crankshaft' pattern of transitivity 1 2 whereas the general case ('gaptooth') (*p*,*q*) gives transitivity 2 2. Examples of woven coordination networks include plain weave[54–57] and a (2,2) twill.[58]

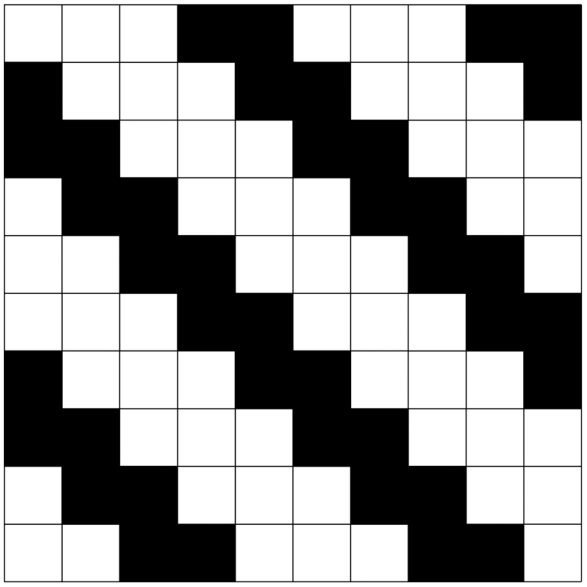

Fig. 7 The design of a (3,2) twill. Horizontal and vertical rows have the sequence three white, two black squares.

3.3 Triaxial weave – kagome

In triaxial weave, three coplanar sets of threads at 120° to each other are woven. It should be clear that isonemal weavings must be balanced [*e.g.* threads (*p*,*p*)]. The simplest, and only regular, has (1,1) threads (*kagome*, Fig. 10). This weave is in a sense analogous to the Borromean rings. There are three sets of threads and no two sets are interwoven. It may be seen in the figure that red is over blue, blue over green, and green over red. A hydrogen bonded structure based on the kagome weave has been reported.[59]

In kagome weave, commonly made with flat ribbons or wooden laths, the plane is not covered. Indeed, *kagome* is Japanese for 'basket eye'. The next simplest triaxial weave, symbol **wvm**, is (3,3) and now the plane can be covered as shown in Fig. 10. This style is known as *mad weave*.[60,61] It has transitivity 1 2 1.

In three-way weave, there could be triple crossings at which three threads meet.[18] Now at a crossing, a thread can be at the bottom (*A*), middle (*B*), or top (*C*). For an isonemal weave *A*, *B* and *C* must occur in equal numbers in a thread so the simplest sequence is *ABCABC*... and this is shown as **wvn** in the figure. It has transitivity 1 2 1.

3.4 Chain-link weave

In the 2-periodic weaves discussed so far, the diagonals between two corners at a crossing are normal to the lattice plane. By contrast in chain-link weaving the diagonals lie in the lattice plane. The two simplest isonemal examples are shown in Fig. 11 and data (symmetry *etc.*) in Table 1. The one with symbol **wvx** is

Published on 04 May 2018. Downloaded by University of California - Berkeley on 6/22/2018 6:56:28 PM.

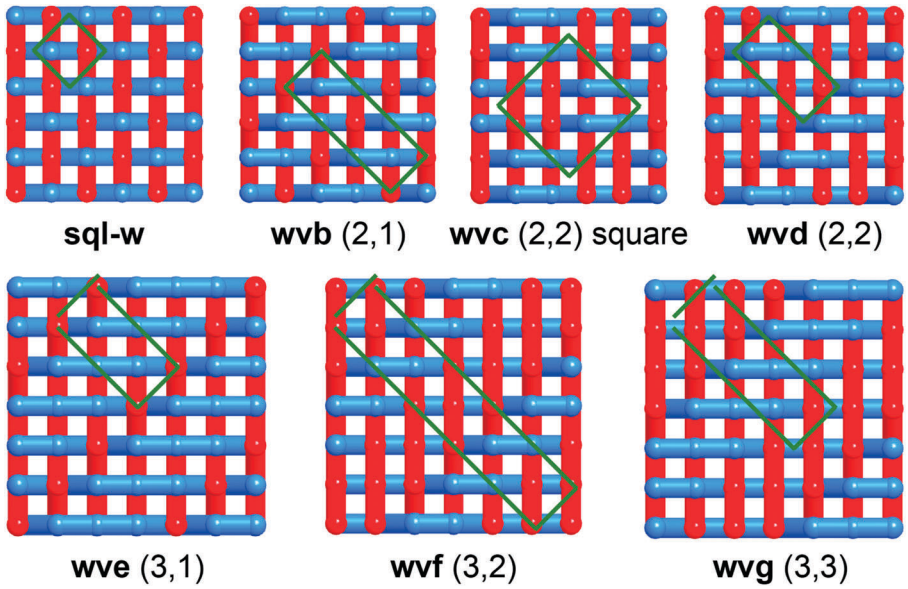

Fig. 8 The simplest biaxial weavings. All but **wvc** are twills.

Table 1 Geometric data for 2-periodic weavings. For fabric weaving (*p*,*q*) after the symbol means for each thread *p* over and *q* under crossings. The entries for stick(s) are the coordinates of corners linked to the corner with coordinates given in the 'corner' column to the left

Symbol	Trans	Symmetry	Cell *a*, *b*	Corner	Stick(s)
wva (1,1)	1 1 1	*p*4/*nbm*	1.414, 1.414	1/4, 1/4, *z*	3/4, 3/4, −*z*
wvb (2,1)	2 2 1	*c*222	1.714, 4.247	0, 0, *z* 0, 0.333, *z*	0.063, 1/2, −*z* 0.167, 1/2, *z*
wvc (2,2)	1 2 1	*p*4/*nbm*	2.828, 2.828	0, 1/4, *z*	1/4, 0, −*z*; −1/4, 0, *z*
wvd (2,2)	1 2 1	*pbaa*	2.818, 1.414	0.375, 1/4, *z*	0.625, 3/4, −*z*; 0.125, −1/4, *z*
wve (3,1)	2 2 1	*p*222	1.414, 2.828	0, 0, *z* 0.25, 1/2, −*z*	0.25, 1/2, −*z*; 0.75, −1/2, −*z*
wvf (3,2)	2 3 1	*c*222	1.414, 7.070	0, 0.2, *z* 0, 0.4, *z*	−1/2, 0.3, *z*; 1/2, 0.1, −*z*; 1, 0.6, *z*
wvg (3,3)	1 2 1	*pban*	4.247, 1.414	0.083, 3/4, *z*	−0.083, 1/4, −*z*; 0.417, 3/4, *z*
kgm-w (1,1)	1 1 1	*p*622	1.0, 1.0	0, 1/2, *z*	1/2, 0, −*z*
wvm (3,3)	1 2 1	*p*622	1.732, 1.732	0.167, 0.833, *z*	0.333, 1.167, −*z*; −0.167, 1.167, *z*
wvx	2 1 1	*c*222	1.4, 2.8	0.15, 0, 0 −0.25, 0.25, *z*	−0.25, 0.25, *z*
wvy	2 2 1	*pban*	1.4, 2.8	0.4, 1/4, 0 1/4, 0.35, *z*	1/4, 0.35, *z*; 1/4, 0.15, −*z*
wvz	1 2 1	*pbam*	3.0, 4.0	0.35, 0.85, −*z*	1.15, 0.85, −*z*; 0.65, 0.15, *z*

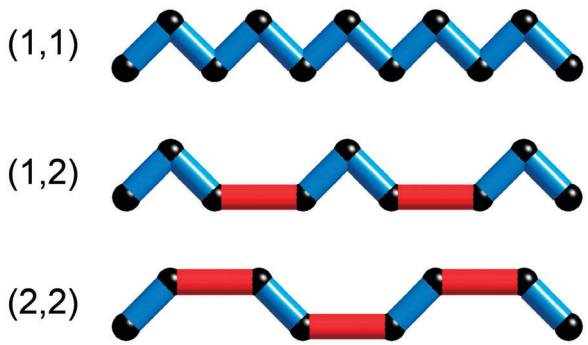

Fig. 9 The shape of one thread in simple weavings. Red and blue sticks are not related by symmetry. (1,1) is 'zigzag' and (2,2) is 'crankshaft'.

most nearly regular with transitivity 2 1 1. It is chiral and the underlying structure of chain-link fences which appear to be always made with right-handed helical threads as shown in the figure. It should be a good target for designed synthesis. Knitting patterns have the same kind of link. The simplest, **wvz**, also shown in Fig. 11, is a variation of 'stockinette' knit. It has transitivity 1 2 1, and again should be a good target for synthesis.

2-Periodic chain-link weaves have been reported in a MOF.[62] They are sometimes referred to as 'chicken wire' but in chicken wire the two-crossing link of chain link is replaced by multiple crossings, typically about 10.

3.5 Two-periodic polycatenanes

In polycatenanes we restrict ourselves first to structures with rings joined by double crossings (Hopf link) to any other ring

 This journal is © The Royal Society of Chemistry 2018

Published on 04 May 2018. Downloaded by University of California - Berkeley on 6/22/2018 6:56:28 PM.

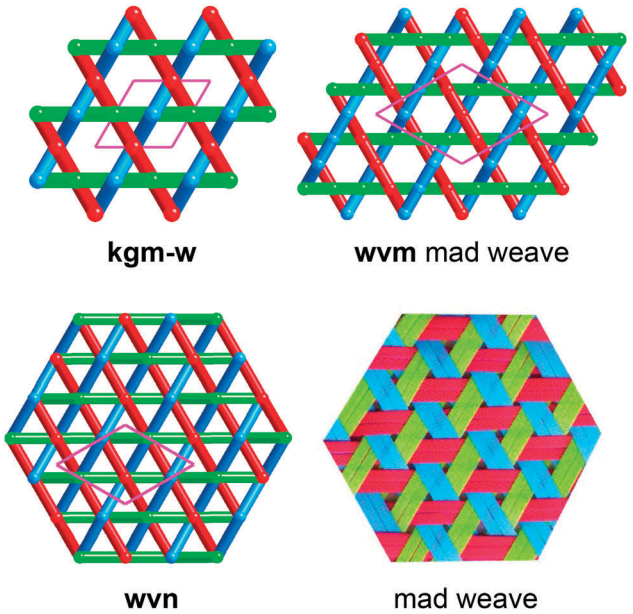

Fig. 10 Simple triaxial weaves. The picture on the bottom right was reproduced from ref. 61 with permission from Taylor and Francis Group copyright, 2017.

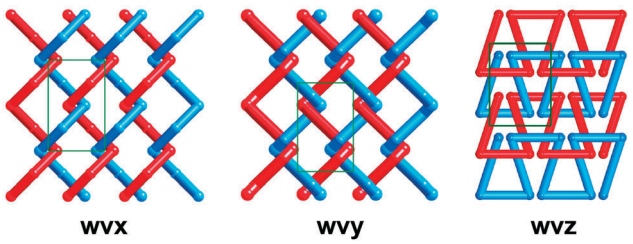

Fig. 11 Left and center the two simplest patterns of chain link. **wvx** is used in fences. Right the stockinette knit, **wvz**.

and to those with just one kind of link point (all link points related by symmetry) and one kind of ring. We consider that these are the most likely targets for designed synthesis. In such structures the link points must be at the vertices of a uninodal (vertex transitive) 4-coordinated (4-c) planar net. There are just three of these: the net, **sql**, of the square lattice (4^4), the kagome net, **kgm** (3.6.3.6), and the 'hexagonal tungsten bronze' net, **htb** (3.4.6.4).

The structures have 3, 4, or 6 crossings per ring. Structural data are collected in Table 2. In the one (**cme**) with 3 crossings per ring, and shown as triangles in projection, the rings have six corners and are in fact nonplanar hexagons. Likewise the rings in the one (**cms**) with six crossings per ring, and derived from **kgm**, are really dodecagons.

There are three structures with 4 crossings per ring and one kind of link point derived from **sql**. The projections shown in Fig. 12 are shown as quadrangles, but in **cmi** and **cmj** they are in fact nonplanar octagons. However, in **cmk** the rings can be planar rectangles. Indeed, this structure with transitivity 1 2 1 is the most nearly regular 2-periodic chainmail. We believe it is the only one that can be made with one kind of planar ring. It is not surprising therefore that it was very commonly used in chainmail armor. In that context it is known as the 'European four-in-one' mail. All other chainmail armor designs we have seen use at least two kinds of ring (*i.e.* not all related by symmetry).

Fig. 13 shows the polycatenanes derived from **htb**. There are two (**cmm** and **cmn**) with four crossings per ring. The rings in the catenanes with 6 crossings per ring are all dodecagons. **cmt** (transitivity 2 1 1) is particularly interesting as it has the Borromean property that no two rings are linked (so we might refer to the link points as 'virtual link points'). The rings cannot be made into (skew) hexagons without sticks intersecting. Interestingly it occurs in a MOF structure[63] in which the angles at one type of corner are very close to 180°. However, intersections are avoided by reducing the symmetry so that there are now two kinds of ring. Anyway, those corners cannot be ignored as they correspond to 2-c metal atoms linking the organic components.

3.6 Some linked knots

We show here (Fig. 14) some simple examples of catenanes that can be considered as linked knots. Data are listed in Table 2. **cka** is linked Solomon links but could also be considered as woven linear chains. **ckb** is linked trefoil knots. **ckc** is linked Borromean rings, but could also be considered as a three-way weave of linear chains. **ckd** is linked David links but could also

Table 2 Geometric data for 2-periodic polycatenanes. The entries under 'link point' are the nets with vertices at the link points. The entries for stick(s) are the coordinates of corners linked to the corner with coordinates given in the 'corner' column to the left

Symbol	Link points	Trans	Sym	Corner	Stick(s)
cme	**kgm**	2 2 1	*p*622	0.583, 0.167, 0 0.583, 0, *z*	0.58, 0, *z*; 0.42, 0.42, −*z*
cmj	**sql**	2 2 1	*p*422	0, 0.3, 0 0.5, 0.8, *z*	−0.2, 0.5, *z*; 0.5, 0.8, *z*
cmi	**sql**	2 1 1	$p\bar{4}2m$	0.3, 0, 0 0.65, 0.35, *z*	0.65, 0.35, *z*
cmk	**sql**	1 2 1	*pbmn*	0.15, 0.15, *z*	0.85, 0.15, −*z*; 0.15, 0.85, *z*
cms	**kgm**	2 1 1	*p*622	0.4, 0, 0 0.6, 0.2, *z*	0.6, 0.2, *z*
cmt	**htb**	2 1 1	$p\bar{3}1m$	0.61, 0.39, 0 0.32, 0, *z*	0.32, 0, *z*
cmu	**htb**	1 2 1	*p*622	0.21, 0.79, *z*	0.58, 0.79, −*z*; −0.21, 0.58, −*z*

Published on 04 May 2018. Downloaded by University of California - Berkeley on 6/22/2018 6:56:28 PM.

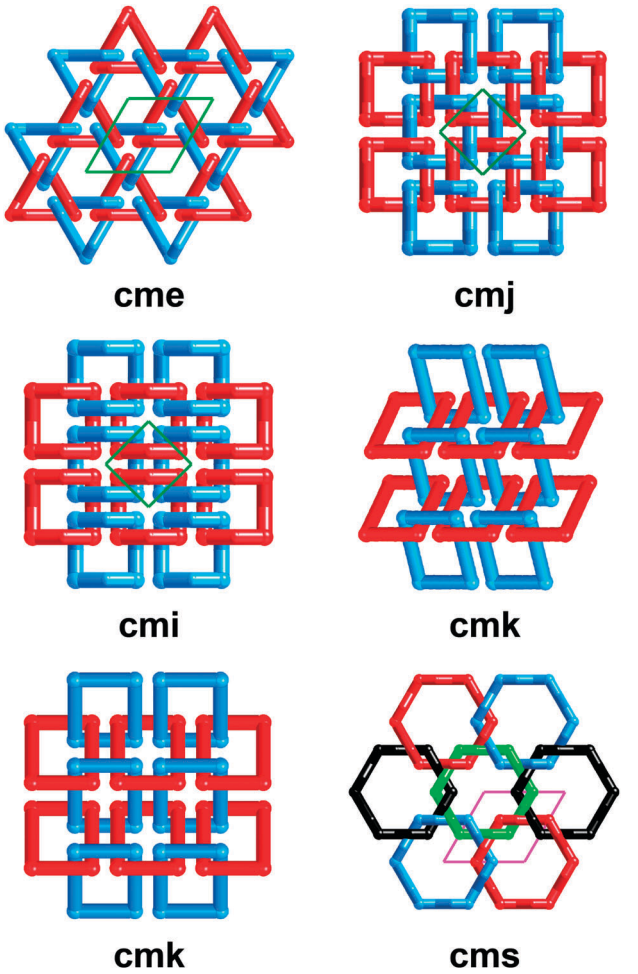

Fig. 12 2-Periodic linked rings with symmetry related link points that form the **kgm** (3.6.3.6) or **sql** (4^4) nets. **cmk** ('European four-in-one chain mail') shown twice is the only one with an embedding with planar rings.

be considered as three interwoven copies of the polycatenane **cme** (Fig. 12).

4. Three-periodic structures

4.1 Description and generation of 3-periodic weavings

4.1.1 Fabric and chain-link weaving and line sets. We do not attempt a formal definition of 3-periodic weaving. But we suggest that a weaving of threads can be recognized by the fact that the threads are interlacing in such a way that they cannot be simultaneously pulled straight without either intersecting or passing through others. We note that a broader definition of "weaving" has been used to describe 3-periodic patterns of helices.[64] None of those structures appear as weavings in this paper. In the 2-periodic weavings of the last section, straightening the threads in fabric weaving leads to the threads intersecting in a vertex-and-edge-transitive 4-c net, either the square lattice net **sql**, or the kagome net **kgm** (Fig. 15). This gives a hint of how to find regular 3-periodic weavings. Thread-weaving structures derived from connected nets, say **abc** we designate **abc-w**. The nets from which the regular fabric weavings are derived will have

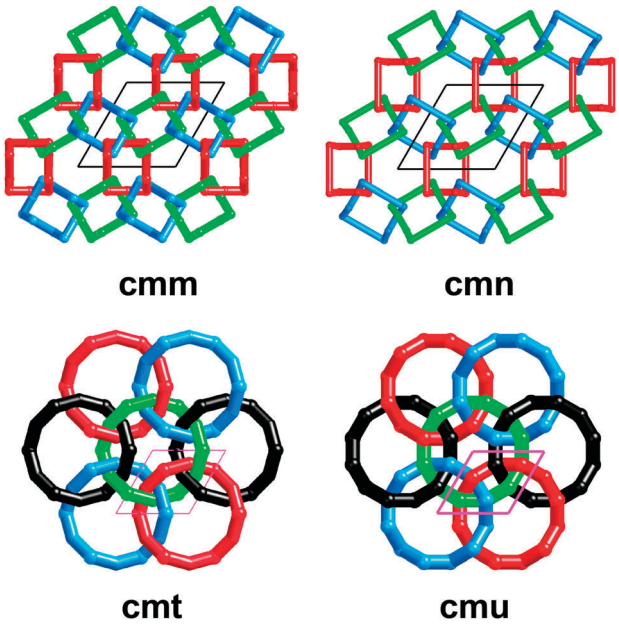

Fig. 13 2-Periodic linked rings with symmetry related link points that form the **htb** (3.4.6.4) net. **cmt** has the Borromean property that no two rings are directly linked.

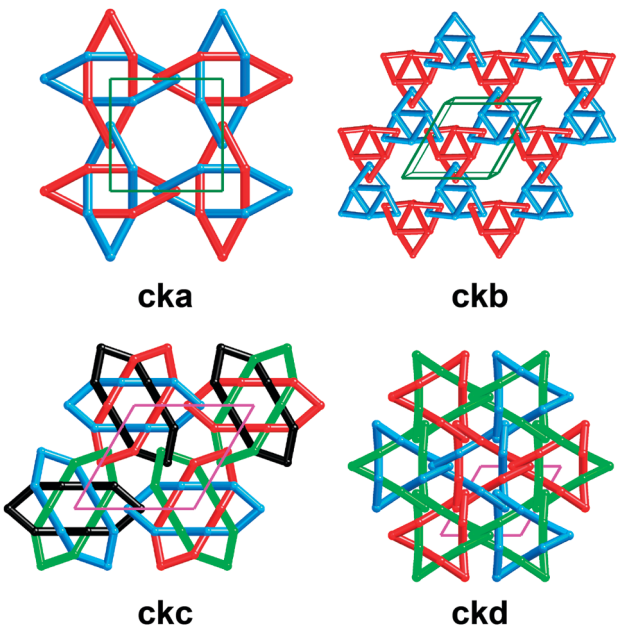

Fig. 14 Examples of linked knots. **cka** is linked Solomon links. **ckb** is linked trefoil knots. **ckc** is linked Borromean rings. **ckd** is linked David links and can also be described as an interpenetration of three **cme** layers (each shown with a different colour).

edges forming straight lines in their symmetric embeddings. The 3-periodic invariant (all coordinates fixed by symmetry) nets formed by intersecting straight lines are listed in Table 3.[65]

In the case of 2-periodic chain-link weaving, straightening threads would require that they pass through each other and form a simple non-intersecting layer pattern. For the regular 3-periodic chain-link weavings the axes of the threads

 This journal is © The Royal Society of Chemistry 2018

Published on 04 May 2018. Downloaded by University of California - Berkeley on 6/22/2018 6:56:28 PM.

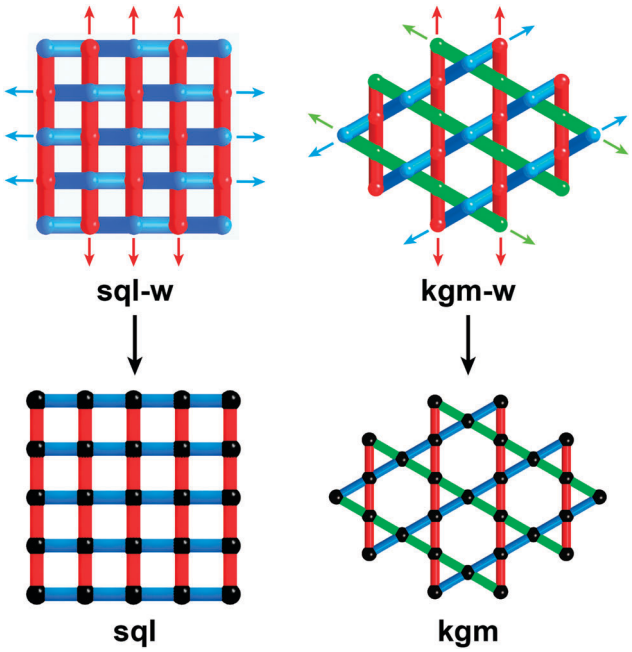

Fig. 15 By pulling the interlacing threads straight in **sql-w** and **kgm-w**, they will collide and intersect to form **sql** and **kgm**, respectively.

Table 3 The 3-periodic invariant intersecting line sets. *pq* indicates that the lines run in *p* directions and *q* intersect at a point. The vertices are 2*q*-coordinated

Type	*pq*	Symbol	Symmetry	Coordinates
Tetragonal 4-way ⟨101⟩	42	**lvt**	$I4_1/amd$	0, 0, 0
Cubic 3-way ⟨100⟩	32	**nbo**	$Im\bar{3}m$	1/2, 0, 0
	33	**pcu**	$Pm\bar{3}m$	0, 0, 0
Cubic 4-way ⟨111⟩	43	**bcs**	$Ia\bar{3}d$	0, 0, 0
	44	**bcu**	$Im\bar{3}m$	0, 0, 0
Cubic 6-way ⟨110⟩	63	**hxg**	$Pn\bar{3}m$	0, 0, 0
	63	**crs**	$Fd\bar{3}m$	0, 0, 0
	64	**reo**	$Pm\bar{3}m$	1/2, 0, 0
	66	**fcu**	$Fm\bar{3}m$	0, 0, 0

will likewise form a 3-dimensional invariant non-intersecting line pattern. These are summarized in Table 4 and illustrated in Fig. 16.[66] In most of the weavings we describe, the axes of the threads form one of these patterns. The idea of 3-periodic chain-link structures has been suggested earlier, and several illustrated, but no geometric or other data given.[67]

In contrast to the 2-periodic case, it is found now that there are many regular (transitivity 1 1 1) chain-link weavings, but we have found only three regular fabric weavings.

4.1.2 Derivation of weavings. We briefly indicate how chain-link weavings are derived from uninodal 4-c nets. Such nets have six angles and the original node is split into 6 (Fig. 17). Two of these, related by symmetry at opposite angles, can be selected to serve corners of a weaving with double crossings. Later we adduce an example of a weaving (**dia-w****) with sextuple crossings. For isogonal (one corner) weavings the original net must be uninodal and have symmetry at the vertex of order at least 2. The RCSR lists 67 such nets, and one net can provide more than one weaving, as we now demonstrate, so the

Table 4 The 3-periodic invariant non-intersecting line sets ('rod packings'). To generate the structure the symmetry operations act on the line in the direction given in the first column passing through a point with the coordinates given

Type	Symbol	Symmetry	Coordinates
1-Way ⟨001⟩	1 **hcb**	*P6mm*	1/3, 2/3, 0
	2 **hxl**	*P6mm*	0, 0, 0
	3 **kgm**	*P6mm*	1/2, 0, 0
	4 **pcu**	*P4mm*	0, 0, 0
2-Way tetragonal ⟨100⟩	5 ϑ	$I4_1/amd$	0, 0, 1/4
	6 Φ	$P4_2/mmc$	0, 0, 0
3-Way hexagonal ⟨010⟩	7 Λ	$P6_222$	1/2, 0, 1/6
3-Way hexagonal ⟨100⟩	8 Δ	$P6_222$	0, 1/2, 0
3-Way cubic ⟨100⟩	9 Π	$I4_132$	1/4, 0, 0
	10 Π^*	$Pm\bar{3}n$	1/2, 0, 0
4-Way cubic ⟨111⟩	11 Σ	$I4_132$	1/3, 2/3, 0
	12 Γ	$Ia\bar{3}d$	0, 0, 0
	13 Ω	$I432$	1/3, 2/3, 0
	14 Σ^*	$Ia\bar{3}d$	1/3, 2/3, 0

number of possibilities is large. Here we indicate how we treated the most symmetric vertex- and edge-transitive nets.

The diamond net, **dia**, at full cubic symmetry ($Fd\bar{3}m$) has six equivalent angles. To remove some of the degeneracy one must go to trigonal or tetragonal symmetry. Trigonal will split into groups of 3, so, to make a weaving with double crossings, the new symmetry must be tetragonal and the maximal tetragonal subgroup is $I4_1/amd$. This splits the 6 into 2 + 4 as shown in the figure. Linking the 2 appropriately gives the regular weaving **dia-w**. The only maximal subgroup of $I4_1/amd$ that splits the group of 4 is $I4_122$, which produces two pairs (Fig. 17). Constructing weavings from these pairs gives an enantiomorphic pair of weavings **dia-w***. By contrast the quartz net, **qtz**, has maximum site symmetry 222 and the angles are already split into three pairs. Each of these leads to a regular weaving **qtz-w**, **qtz-w***, and **qtz-w****.

The sodalite net, **sod**, illustrates another feature. At full symmetry ($Im\bar{3}m$) the site symmetry is $\bar{4}2m$ and the angles are split into 4 + 2. Linking corners corresponding to the unique pair give a regular polycatenane of linked squares, **sod-y**. Lowering the symmetry to $Pn\bar{3}m$ splits the four into two pairs, each of which gives the regular polycatenane **sod-y*** of linked hexagons. These results show the close relation between weavings and polycatenanes. However, a different maximal subgroup of $Im\bar{3}m$, namely $I432$, again splits the group of four into two pairs and these give enantiomorphs of a regular chiral weave **sod-w**. Nets with planar 4-coordination (*e.g.* **nbo**) are not amenable to this treatment but a regular fabric weave **nbo-w** has been found. In contrast to the 2-periodic case, regular 3-periodic weaves with triple crossings are possible. We find **pcu-w**, **pcu-w***, **crs-w**, **acs-w**, and **lcy-w** all derived from vertex- and edge-transitive 6-c nets. Just one regular weaving with quadruple crossings has been found – **thp-w** derived from the 8-c net **thp**.

4.1.3 Optimal embedding and girth. Knot theorists determine an 'ideal' embedding of a finite knot as that which uses the shortest length of a rope of fixed width. The 'energy' that is minimized is the ratio of rope length to diameter.[68] A recent paper, which gives a comprehensive review, shows how such a procedure can be applied to periodic systems.[69]

Published on 04 May 2018. Downloaded by University of California - Berkeley on 6/22/2018 6:56:28 PM.

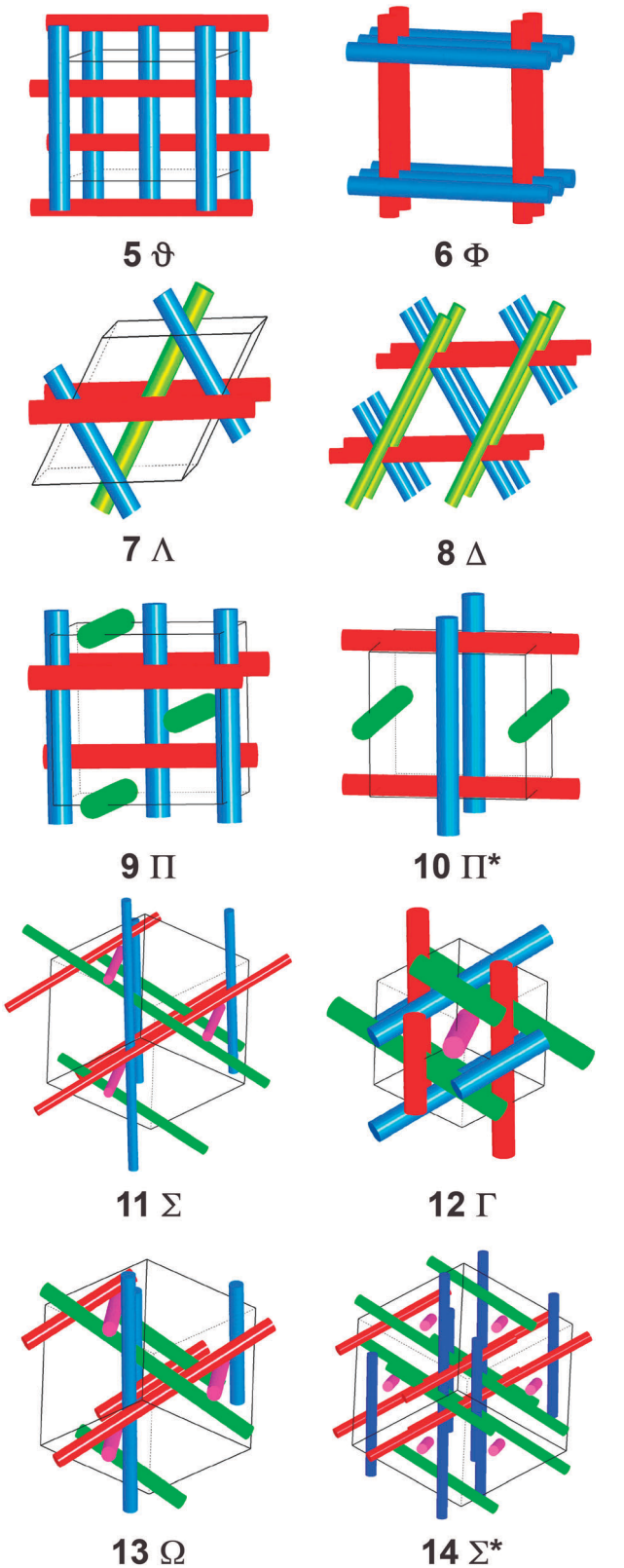

Fig. 16 The invariant rod packings with the numbers and symbols of Table 4.

In this work, we use a related procedure to find an optimal embedding for piecewise linear weavings. For weavings of

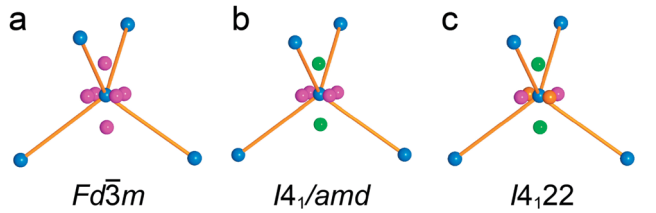

Fig. 17 (a) Six symmetry-related points at a vertex of the diamond (**dia**) net with symmetry $Fd\bar{3}m$. (b) With symmetry $I4_1/amd$ the points are split into sets of 2 and 4 symmetry-related points. (c) With symmetry $I4_122$ the points are further split into 3 groups of 2.

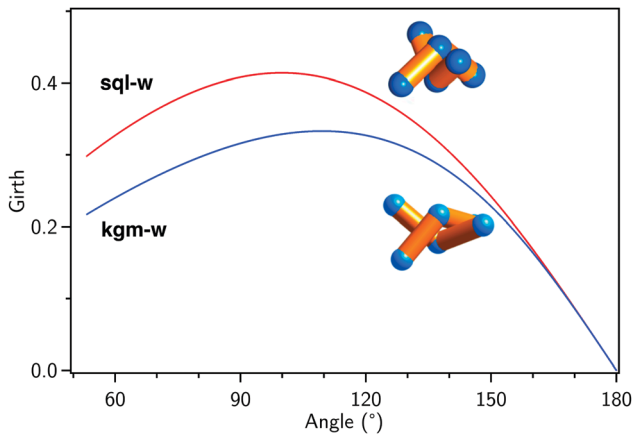

Fig. 18 Girth as a function of the angle at a corner (corner angle) between two contiguous sticks for the regular 2-periodic weavings **sql-w** and **kgm-w**. The crossings shown are for maximum girth.

threads containing just one kind of cylindrical stick we find the width of the cylinder that brings a stick into contact with one or more neighbors. The *girth* of a stick is then the ratio of that width to the stick length. The optimal embedding is the one that maximizes the girth of non-intersecting sticks.

In Fig. 18, notable is a broad maximum in each case. The maxima are at:

$$\textbf{sql} - \textbf{w}\ \text{girth} = 0.414\ \text{at}\ 99.9^\circ\ \ (\sqrt{2}-1,\ 2\ \tan^{-1}\ 2^{1/4})$$

$$\textbf{kgm-w}\ \text{girth} = 0.333\ \text{at}\ 109.5^\circ\ [1/3,\ \cos^{-1}(-1/3)]$$

We consider that the greater the maximum girth the more amenable to synthesis will be a weaving composed of polyatomic threads. The broad maximum, which is characteristic of the weavings we have studied, indicates that the angle at a corner is not critical in determining a weaving. We have found optimal embeddings for the regular 3-periodic weavings and numerical data are reported below. For structures with transitivity other than 1 1 1, the reported embedding is not optimal, but adequate to specify the structure. However, we note that such optimal embeddings could be found for all the structures in this article.

4.2 3-Periodic fabric weaving

We have examined the nets of the invariant intersecting line set (Table 3) as sources of fabric weaving. The two with 4-c vertices

 This journal is © The Royal Society of Chemistry 2018

Published on 04 May 2018. Downloaded by University of California - Berkeley on 6/22/2018 6:56:28 PM.

Table 5 Generation of regular chain-link weavings and catenanes. The original nets are 4-c except for **acs** (6-c). For these last two we show first the symmetry of the net, then that of the weaving

Parent	Symmetry	Angles	
dia	$Fd\bar{3}m$	(6)	—
	$I4_1/amd$	(4) + 2	**dia-w** zigzag
	$I4_122$	(2) + 2 + 2	**dia-w*** 4_1 and 4_3 helices
qtz	$P6_222$	2 + (2 + 2)	**qtz-w** zigzag
		(2) + 2 + (2)	**qtz-w*** 3_2 helices
		(2 + 2) + 2	**qtz-w**** 6_2 helices
sod	$Im\bar{3}m$	(4) + 2	Catenated 4-rings
	$Pn\bar{3}$m	(2) + 2 + 2	Catenated 6-rings
	$I432$	(2) + 3 + 3	**sod-w** 3_1 and 3_2 helices
lcs	$Ia\bar{3}d$	(4) + 2	**lcs-w** 4_1 and 4_3 helices
	$I4_132$	(2) + 2 + 2	**lcs-w*** two sticks
lcv	$I4_132$	2 + (2 + 2)	Catenated 3-rings
		(2) + 2 + 2	**lcv-w** 3_1 or 3_2 helices
ana	$Ia\bar{3}d$	(1 + 1 + 2) + 2	Catenated 4-rings
		(1 + 1) + 2 (+2)	Catenated 6-rings
acs	$P6_3/mmc$	→ $P6_322$	**acs-w** 6_1 or 6_5 helices

(**nbo** and **lvt**) give fabric weaves with one kind of crossing point. There are four of these nets with 6-c vertices. Two (**pcu** and **crs**) yield fabric weaves with triple crossing points. Geometric data for these weavings are given in Table 5.

nbo-w. The **nbo** net is the only one with full square symmetry ($4/mmm = D_{4h}$) at the vertex and the derived weave, **nbo-w** (Fig. 19), and is the only regular (transitivity 1 1 1) fabric weave we have found with two-way crossings. At the optimal embedding, girth = 0.619, corner angle = 139°. The threads are 4_1 and 4_3 helices and threads of one hand are directly linked only to threads of opposite hand. Interwoven helical SBUs based on this pattern have been identified in rod MOFs but in those materials the rods are linked by polytopic linkers so the structure is not a weaving.[65]

cds-w. All other 4-c nets with embeddings in which all vertices are in square coordination are at least edge 2-transitive so cannot yield isonemal weavings. The simplest such net is **cds** and the corresponding weaving **cds-w** (Fig. 20) which has symmetry $F4_12_12$ and transitivity 4 4 2 (each thread 2 2 1).

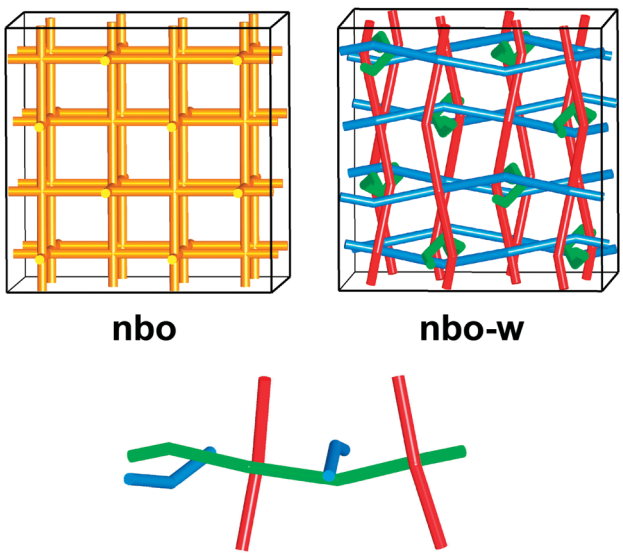

Fig. 19 The **nbo-w** fabric weave. On the left is shown the structure of the intersecting thread axes, below is shown one helical thread and the links with red and blue threads.

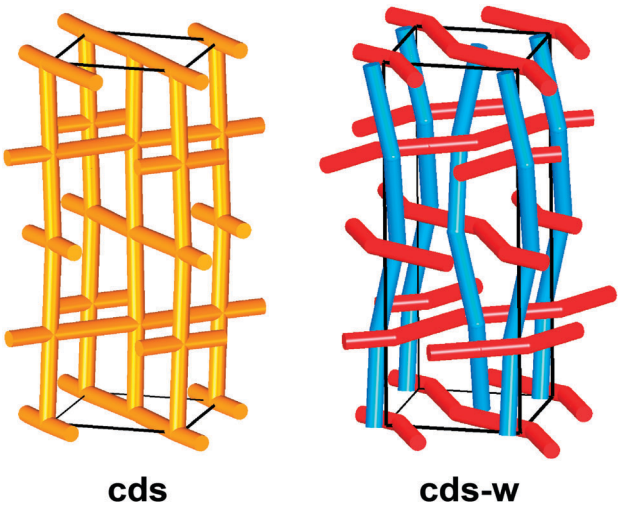

Fig. 20 A weaving derived from the **cds** net shown on left.

lvt-w. The **lvt** net, the other invariant 4-c net formed from intersecting; it yields **lvt-w** (Fig. 21) but the best embedding we can find has transitivity 1 2 1.

pcu-w. The 3-periodic analog of the simple regular 2-periodic two-way weaving has zigzag threads running in three perpendicular directions. This is the regular weaving **pcu-w** (Fig. 22). Presumably there is a family of less-regular weavings just as in the 2-periodic case – we have not explored this. In the optimal embedding girth = 0.253, corner angle = 94.6°.

crs-w. This (Fig. 23), like **pcu-w**, is a chiral regular weaving with triple crossings and zigzag threads. It was suggested by examination of nets formed from linked helical ladders.[70] In the optimal embedding girth = 0.277, corner angle = 108.3° (Table 6).

4.3 3-Periodic chain-link weaving

In contrast to the 2-periodic case, there are many different kinds of chain-link weaving. Accordingly, for isonemal weavings we generally restrict ourselves to regular ones.

4.3.1 Parallel helical threads. Here we describe some isonemal and dinemal (two kinds of thread) with respectively

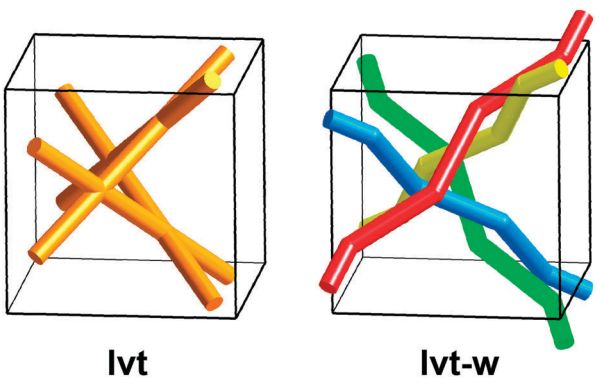

Fig. 21 A fabric weave (right) derived from the **lvt** net (left).

Published on 04 May 2018. Downloaded by University of California - Berkeley on 6/22/2018 6:56:28 PM.

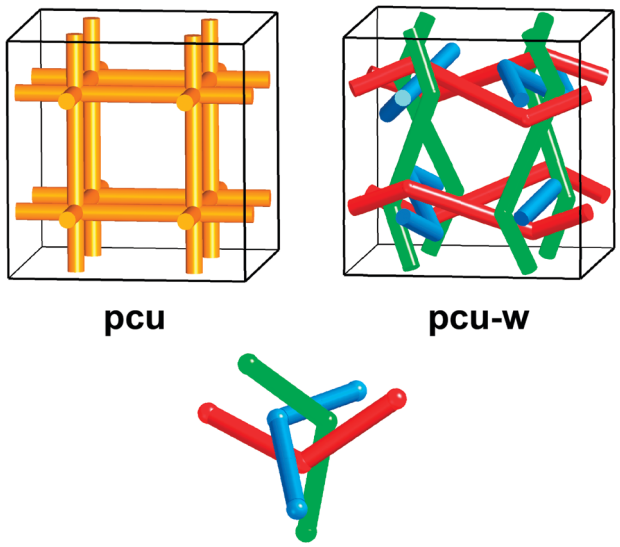

Fig. 22 A fabric weave (top right) derived from the **pcu** net (top left). On the bottom is a detail in the vicinity of a triple crossing link point.

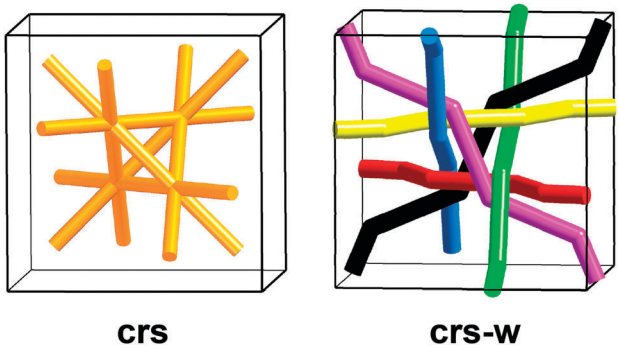

Fig. 23 The **crs** net and the derived fabric weave with triple crossing link points.

transitivity 1 1 1 and 2 2 2. For isonemal weavings only chiral structures appear possible. Geometrical data are recorded in Table 7.

dia-w*. This (Fig. 24) is one of two isonemal structures derivable from the diamond (**dia**) net with either linked 4_1 or 4_3 helices. The optimal embedding has a simple exact solution – the girth is $1/\sqrt{6} = 0.408$, the axial ratio c/a is $2\sqrt{2}$ and the corner angle is $\cos^{-1}(-1/3) = 109.5^\circ$. The diamond net is particularly amenable to forming interpenetrating pairs and also shown is the structure **dia-w*-c** with two interpenetrating weavings.

qtz-w*. This (Fig. 25) is the corresponding weaving of 3_1 or 3_2 helices. In the optimal embedding, girth = 0.310, c/a = 1.88, corner angle = 78.5°. Quartz nets of the same hand also readily interpenetrate, and also shown in the figure is the interpenetrating weaving.

qtz-w**. This (Fig. 26) is another of the three isonemal weaving derived from the quartz net. Now the threads are 6_1 or 6_5 helices. At the optimal embedding girth = 0.450, c/a = 1.41, corner angle = 129.6°. Note that there are two separate coaxial

Table 6 Geometric data for 3-periodic fabric weaving. In the 'stick' column, that vertex is linked to the one in the 'corner' column. All have transitivity 1 1 1 except **lvt-w** (1 2 1)

Symbol	Symmetry	Corner	Stick
nbo-w	$Fd\bar{3}c$	7/8, 7/8, −0.024	1/8, 0.774, 1/8
lvt-w	$I4_122$	0.5, 0.7, 0.68	0.2, 1.0, 0.83; 0.7, 0.5, 0.33
pcu-w	$I432$	3/4, 0.413, 0.087	1/4, 0.087, 0.413
crs-w	$F4_132$	0.29, 0.46, 5/8	0.71, 0.54, 5/8

Table 7 Geometric data for 3-periodic chain-link weaving with parallel threads. In the 'stick' column, that vertex is linked to the one in the 'corner' column. The transitivity is 1 1 1 or 2 2 2; in the latter case, there are two rows per structure

Symbol	Symmetry	Corner	Stick
dia-w*	$I4_122$	0.25, 0.25, 0	0.25, −0.75, 1/4
dia-w*-c	$P4_222$	0.0, 0.3, 0.5	0.7, 1.0, 0.0
qtz-w*	$P6_222$	0.25, $1-x$, 1/3	$2x-1$, x, 2/3
qtz-w*-c	$P6_222$	0.44, 0.88, 0	0.44, 1.16, 1/3
qtz-w**	$P6_222$	0.764, 0, 0	0.764, 0.764, 1/3
acs-w	$P6_322$	1, −0.505, 1/4	1.01, 1.505, 3/4
unc-w	$P4_122$	0.44, 0, 3/4	0, 0.56, 1/2
		0, 0.22, 0	0, 0.78, 1/2
und-w	$I4_1/amd$	3/4, 0.4, 0	3/4, 0.1, 1/2
		1/4, 0.28, 1/2	0.47, 1/2, 1/4
unh-w	$P6_122$	0.48, 0.96, 0.25	0.48, 0.52, 0.92
		0.38, 0.76, 0.25	0.62, 0.25, 0.75
ung-w	$R\bar{3}c$	0, 0.47, 1/4	0.14, 1/3, 7/12
		0, 0.39, 1/4	0, 0.61, 3/4
uni-w	$P6_122$	0.46, 0, 0	0.46, 0.46, 1/6
		0.32, 0, 0	0.68, 0, 1/2
unj-w	$P6_122$	0.32, 0.16, 1/12	0.84, 0.16, 5/12
		0.31, 0.62, 1/4	0.62, 0.31, 1/12

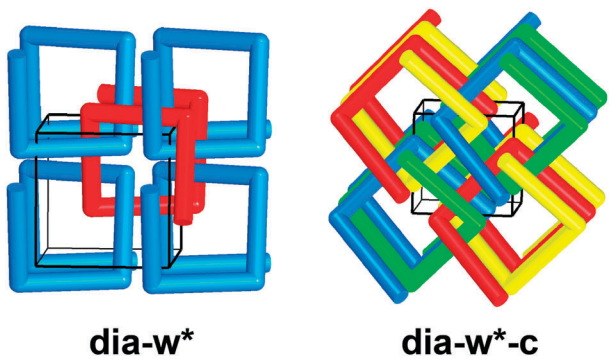

Fig. 24 Left: A chain-link weaving of tetragonal helices derived from the diamond (**dia**) net. Right: Two such interpenetrating weavings.

helices that are not directly linked. With reference to the figure it may be seen that green and blue are coaxial, and that green is linked to black, black to yellow, and yellow to blue. We emphasize that there is just one kind of helix – indeed there is just one helix per unit cell in the sense that all are related by translations.

acs-w. This (Fig. 27) is a nice example of a weaving with a triple crossing (see figure). At the optimal embedding girth = 0.315, c/a = 1.50, corner angle = 135.6°. Now there are three coaxial 6_1 or 6_5 helical threads that are not directly linked. Each of the three is linked to two of the three in neighboring

This journal is © The Royal Society of Chemistry 2018

Published on 04 May 2018. Downloaded by University of California - Berkeley on 6/22/2018 6:56:28 PM.

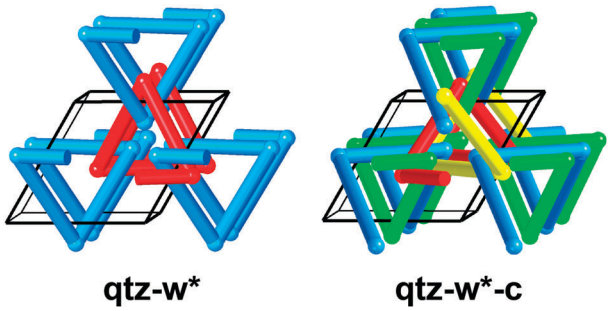

Fig. 25 Left: A chain-link weaving of trigonal helices derived from the quartz (**qtz**) net. Right: Two such interpenetrating weavings.

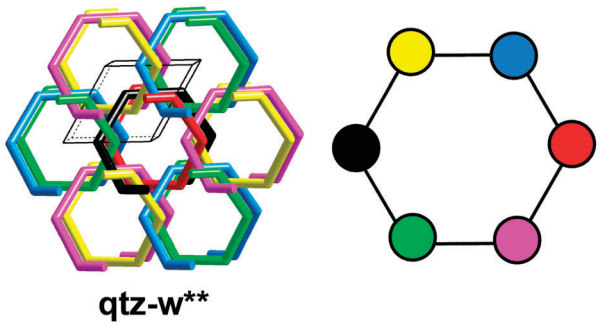

Fig. 26 Left: A chain-link weaving of hexagonal helices derived from the quartz (**qtz**) net. The pattern on the right shows how the helices are linked. Helices are linked to those of neighboring colours; for example, blue is linked to red and yellow. Coaxial helices have colours on a diameter of the hexagon; for example, blue and green.

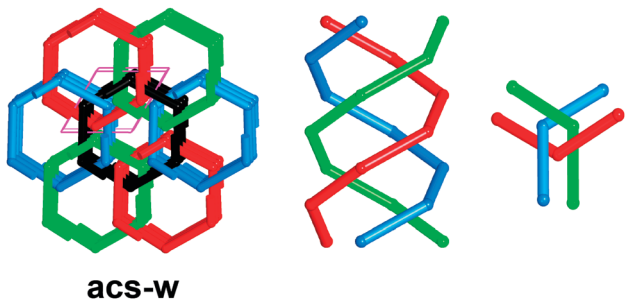

Fig. 27 Left: A chain-link weaving derived from the 6-c **acs** net. As shown in the middle, each column is actually three coaxial helices. Right shows the vicinity of a triple crossing link point. Note that colours do not have the same significance in the different panels.

columns so the whole assembly forms just one weaving – as we know it must – as the net of link points (**acs**) is a connected net. Again, there is just one helix per unit cell.

We also show (Fig. 28) some dinemal weaving of parallel helices. The transitivity in each case is 2 2 2 – the minimum for a dinemal weaving. Importantly, from the design point of view, in each case there is just one kind of link point. Zigzag threads can link trigonal helices of opposite (**unc-w**) or the same (**und-w**) hands. Likewise zigzags can link tetragonal helices of opposite (**unh-w**) or the same (**ung-w**) hands. It should be clear from the figure that zigzags can only link hexagonal helices of the same

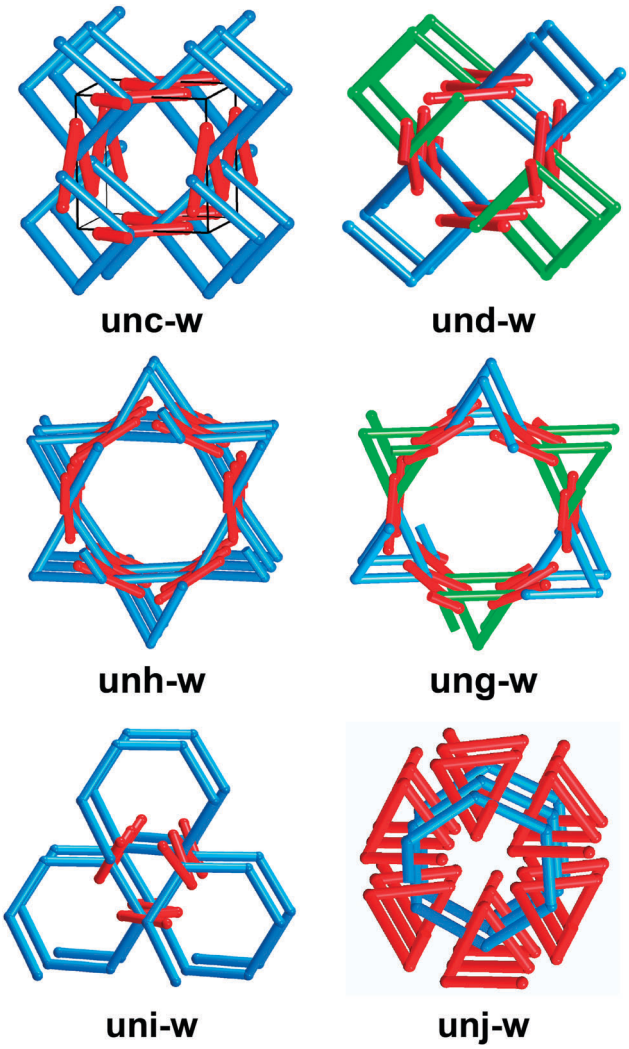

Fig. 28 A series of weavings of two kinds of parallel threads and transitivity 2 2 2. Top four: Zigzag + helix. Bottom two: Two helices.

hand (**uni-w**). Finally in the figure is a linkage of trigonal and hexagonal helices (**unj-w**). In this chiral pattern 3_1 and 6_1 (or 3_2 and 6_5) helices are linked.

4.3.2 Chain-linked zigzag threads in layers. qtz-w and **dia-w.** Here we recognize two special structures with threads whose axes lie in parallel layers. They are derived from the quartz (**qtz**) and diamond (**dia**) nets by splitting the 4-c vertices as describer earlier (Section 4.1.2). **dia-w** is notable for the fact that the threads cross at right angles making them particularly favorable for designed synthesis of 3-periodic weaving with zigzag threads in crystals and indeed the structure of the 3-periodic weavings (COF-505[71] and COF-112[72]) reported to date are based on **dia-w** (Fig. 29). At the optimal embedding for **dia-w** girth = 0.294, c/a = 0.52, corner angle = 95.4°. For **qtz-w** girth = 0.293, c/a = 0.40, corner angle = 104.5°. Data (symmetry, coordinates) are to be found in Table 8.

The structures are illustrated in Fig. 30. **dia-w**, is particularly amenable into forming two interpenetrating structures **dia-w-c**. The symmetry goes from $I4_1/amd$ to $P4_2/nnm$. In both cases four

Published on 04 May 2018. Downloaded by University of California - Berkeley on 6/22/2018 6:56:28 PM.

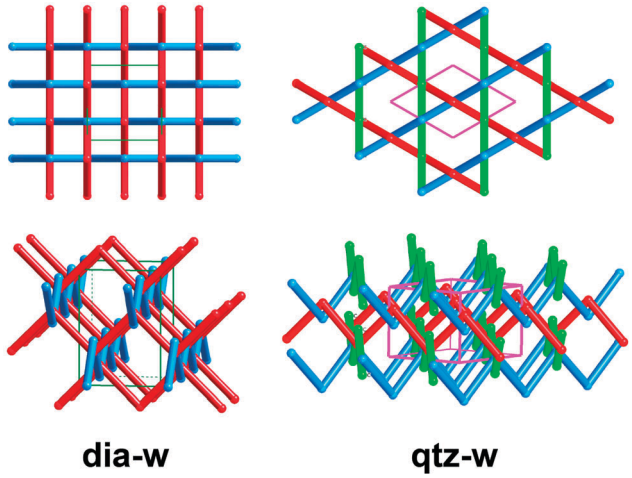

Fig. 29 Left: Two views of the **dia-w** chain-link weave derived from the diamond (**dia**) net. Right: Two views of the **qtz-w** chain-link weave derived from the quartz (**qtz**) net.

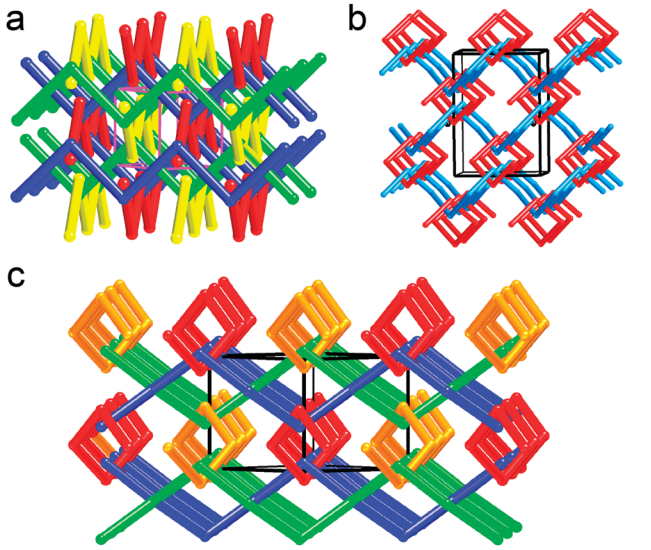

Fig. 30 Variation on the **dia-w** weaving of Fig. 28. (a) Two interpenetrating weavings. (b) The basic weaving with the zigzags replaced by helices. (c) Two interpenetrating copies of the structure in (b). Red and blue helices are linked together by the yellow and green ones. This is the underlying structure of COF-505.[71]

Table 8 Geometric data for 3-periodic chain-link weaving with non-parallel threads. In the 'stick' column, that vertex is linked to the one in the 'corner' column. Under 'thread' is the shape (2_1 is zigzag) and the symbol for the packing (Fig. 16). All have transitivity 1 1 1 except **pts-w** (2 1 1) and **hbo-w** (1 2 1)

Symbol	Symmetry	Corner	Stick	Thread
dia-w	$I4_1/amd$	0, 3/4, 0.434	0, 1/4, 0.434	2_1 ϑ
dia-w-c	$P4_2/nnm$	1/4, 3/4, 0.85	−1/4, 1/4, 0.15	2_1 Φ
qtz-w	$P6_222$	1/2, 1/2, 0.008	0, 1/2, 0.992	2_1 Λ
pts-w	$P4_122$	0, 0, 0.17	−1/2, 0.12, 1/2	2_1 Φ
sod-w	$I432$	0.069, 1/4, 0.431	−0.069, 0.569, 3/4	3_1 Ω
lcs-w	$Ia\bar{3}d$	3/4, 0.488, 0	3/4, 0.512, −1/4	$4_{1,3}$ Π*
lcv-w	$I4_132$	0.458, 0.708, 5/8	0.792, 5/8, 0.542	3_1 Σ
lcv-w*	$I4_132$	0.075, 0, 1/4	1/4, 0.175, 0	3_1 Σ
lcy-w	$P4_132$	3/8, 1.539, 0.211	0.461, 0.711, 1/8	3_1 Σ
lcy-w*	$P4_132$	7/8, −0.008, 0.742	3/8, 0.508, 0.242	2_1 Π
thp-w	$I\bar{4}3d$	0.80, 0.18, 0.03	0.32, 0.03, 0.20	3_1 Γ
dia-w**	$F4_132$	1/4, 1/4, 0.63	0.62, 0, 0	4_1 Π*
hbo-w	$Pm\bar{3}n$	0.62, 0.29, 0.83	0.32, 0.29, 1.17	—

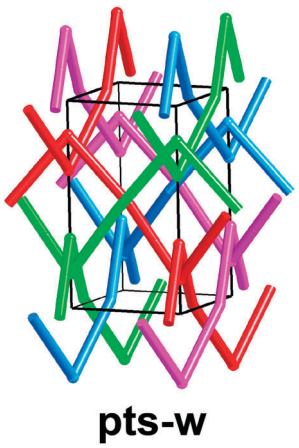

Fig. 31 Decomposing the **pts** net into threads. Threads of one color constitute a **dia-w** weaving.

link points per primitive cell. Of interest with respect to real materials is the symmetry of the zigzag threads, which are replaced by 4-fold helices. Then one gets a structure with interwoven 4_1 and 4_3 helices as shown in Fig. 31. Finally, interpenetrating two such structures gives an idealization of the actual structure of COF-505. The symmetries are now $I\bar{4}2d$ and $P\bar{4}n2$ (interpenetrated pair), and COF-112 has the non-interpenetrated structure. COF-505 has the interpenetrated structure.

We show here also structures derived from the tetragonal net **pts**, the simplest structure with both planar and tetrahedral 4-c vertices. Splitting the tetrahedral vertices in chain-link fashion results in linked rods running normal to the tetragonal axis. Splitting also the planar vertices in fabric-weave fashion produces a weaving of threads (Fig. 31). As shown in the figure, the structure can be considered a weaving (interpenetration) of four **dia-w** weaves.

4.3.3 Cubic chain-link weaves. Here we describe regular isonemal chain-link weavings with thread axes running in three directions (cubic ⟨100⟩) or four directions (cubic ⟨111⟩). For the most symmetrical, the pattern of axes is one of the invariant ones illustrated in Fig. 16.

sod-w. This (Fig. 32) structure is formed by 3_1 (or 3_2) helices with axes in the Ω pattern. Twelve threads combine to weave the cage (tile) shown. In the optimal embedding girth = 0.152, corner angle = 93.6°.

lcs-w. In this structure (Fig. 33), threads are 4_1 and 4_3 helices with axes forming the Π* pattern with a doubled cell to allow ordering of the 4_1 and 4_3 helices as shown in the figure. As in **nbo-w**, direct links are only between helices of opposite hand. In the optimal embedding girth = 0.429, corner angle = 108.2°.

lcv-w and **lcv-w*** (Fig. 34). These are more chiral structures with two degrees of freedom. In **lcv-w** the corners in x, x + 1/4,

 This journal is © The Royal Society of Chemistry 2018

Published on 04 May 2018. Downloaded by University of California - Berkeley on 6/22/2018 6:56:28 PM.

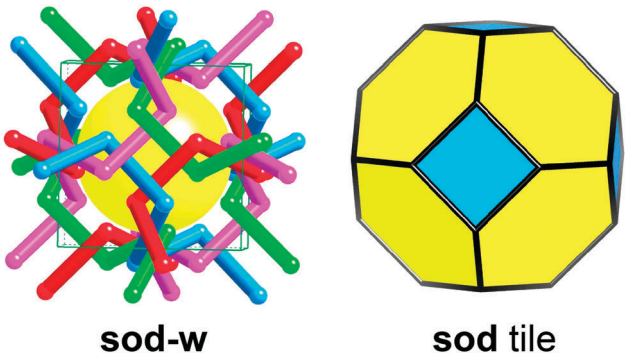

Fig. 32 Left: **sod-w**. Parallel threads (trigonal helices) have the same colour. Twelve threads combine to make the space-filling cage shown.

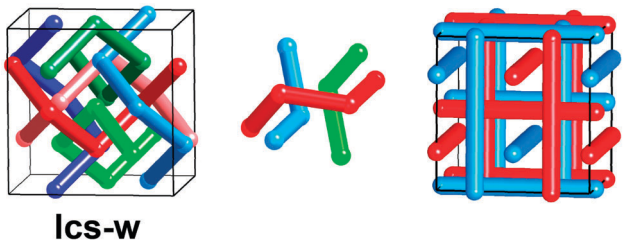

Fig. 33 Aspects of the **lcs-w** chain-link weaving of tetragonal helices. Directly linked helices are of opposite hand. Middle: A close-up of the pattern of linking. Right: The pattern of helix axes. Red and blue rods correspond to helices of opposite hand and form a superstructure of the Π* packing (Fig. 16).

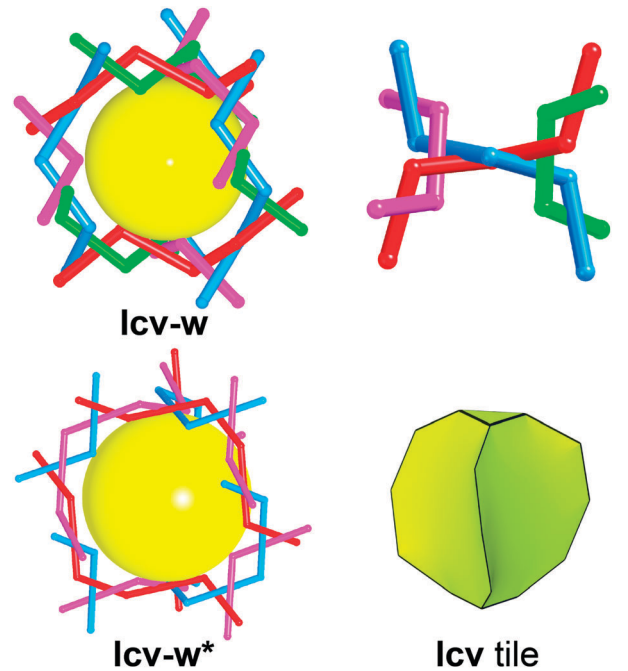

Fig. 34 The **lcv-w** and **lcv-w*** weavings corresponding to a tile of the structure, shown on the lower right. Threads of the same color are parallel. In **lcv-w** they run along ⟨111⟩ and in **lcv-w*** they run along ⟨100⟩.

1/8 and the threads are 3_1 (or 3_2) helices in the Σ pattern. In **lcv-w*** the corners in x, 0, 1/4 and the threads are 4_1 (or 4_3) helices in

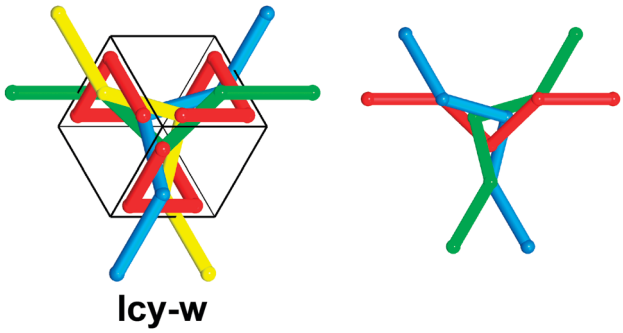

Fig. 35 **lcy-w**. Chain-link weaving derived from the 6-c net **lcv**. Detail in the vicinity of a triple-crossing link point is shown on the right.

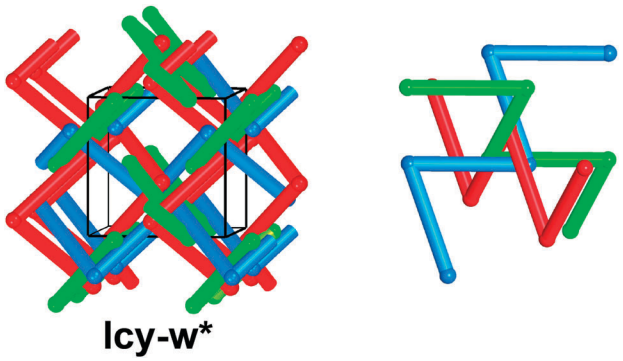

Fig. 36 **lcy-w***. A second chain-link weaving derived from **lcv** compared with **lcv-w** (Fig. 34).

the Π pattern. This latter weaving accommodates only narrower threads. In the optimal embedding for **lcv-w** girth = 0.142, corner angle = 124.6°; for **lcv-w*** girth = 0.082, corner angle = 147.9°.

lcy-w. **lcy** (Fig. 35) is a 6-c net, so a triple-crossing link point (shown in the figure) is necessary. Again, the threads are 3_1 (or 3_2) helices in the Σ pattern. In the optimal embedding the girth = 0.252, corner angle = 108.3°.

lcy-w*. The corners of **lcy-w** (Fig. 36) can be connected differently to obtain a new weaving of zigzag threads. The threads run along ⟨100⟩ and their axes are arranged in a lower-symmetry version of the Π packing. In the optimal embedding girth = 0.104, corner angle = 68.8°.

pcu-w*. This structure (Fig. 37) is another weaving with triple crossings and of interest in several ways. It is a chain-link weaving with link points at the vertices of a **pcu** net. – contrast with **pcu-w**, which is a triple-crossing fabric weave with the same pattern of link points. The threads are 3_1 (or 3_2) helices with axes forming the same pattern as in **sod-w**. In fact, all three weaves (**pcu-w**, **pcu-w*** and **sod-w**) have the same symmetry (*I*432) and corners in the same Wyckoff set (x, x + 1/2, 1/4), The difference between the three weavings is that the stick corners are different pairs of coordinates.

For the optimal embedding of **pcu-w*** girth = 0.077, corner angle = 74.2°.

thp-w. **thp** (Fig. 38) is an 8-c net so the derived weaving has a quadruple-crossing link point as shown in the figure. The full structure is hard to depict clearly and we just show the proximity of a link point and the thread packing. The threads

Published on 04 May 2018. Downloaded by University of California - Berkeley on 6/22/2018 6:56:28 PM.

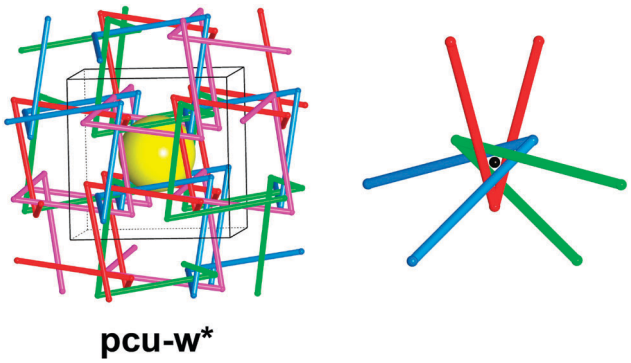

Fig. 37 The **pcu-w*** weaving. Parallel threads have the same colour. On the left are shown 12 helices enclosing the yellow sphere at the center – compare **sod-w** (Fig. 31). On the right are shown three threads in the vicinity of a link point (black sphere).

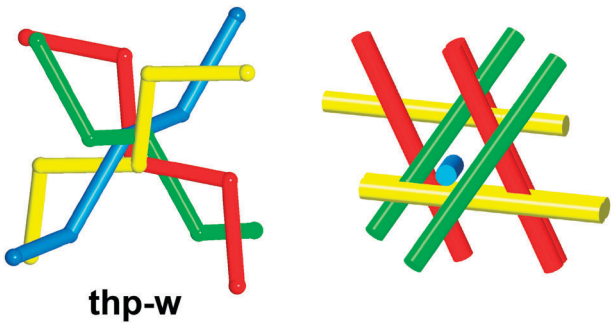

Fig. 38 **thp-w**. Left: A fragment of a chain-link weaving derived from the 8-c net **thp**. Right: The pattern of the helical thread axes.

are zigzags running along ⟨111⟩ and the pattern of their axes is a supercell (2 × 2 × 2) of the Γ packing in a lower-symmetry arrangement, as shown in the figure. For the optimal embedding, girth = 0.111, corner angle = 86.4°.

dia-w**. This weaving (Fig. 39) is shown as an example of a weaving with sextuple crossings. The six symmetry-related points around a vertex in the **dia** (diamond) net are still related by symmetry in $F4_132$ and can be linked to make a weaving as

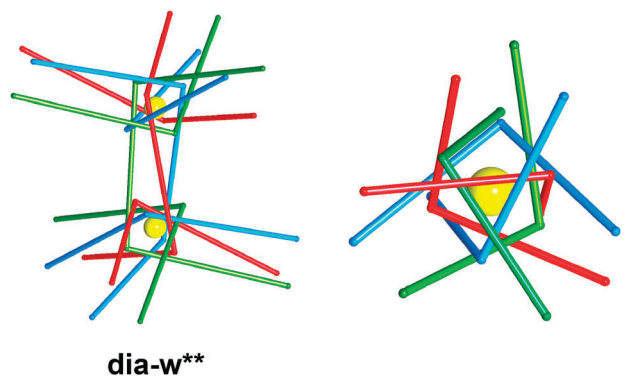

Fig. 39 Two aspects of the **dia-w**** weaving. Left: Showing how corners at two crossing points are linked by three sticks. Yellow balls are at the vertices of the parent **dia** net. Right: Close-up of one sextuple crossing at the optimal embedding. Threads of the same color are parallel.

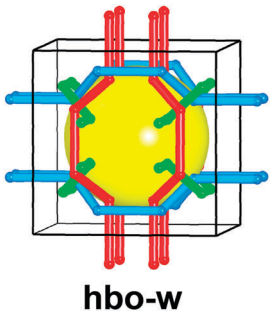

Fig. 40 **hbo-w**. A chain-link weaving of crankshaft threads derived from the 4-c net **hbo** with transitivity 1 2 1. Twelve threads combine to form the cavity centered by the yellow ball.

shown in the figure. There it can be seen that each edge of the parent **dia** net is replaced by three sticks. The threads are 4_1 (or 4_3) helices with axes forming the Π* pattern with a doubled cell as in **lcs-w**, but now all helices of the same hand. As might be expected for a structure with a high number of crossings, the weaving is only possible with narrow threads. At the optimal embedding girth = 0.051, corner angle = 94.2°.

hbo-w. This (Fig. 40) is an example of an isonemal weaving with crankshaft threads. Though not regular (the transitivity is 1 2 1) it should be a credible candidate for designed synthesis.

4.4 Polycatenanes

Polycatenanes (linked rings) are readily derived from 4-c nets and we use a symbol **abc-y** for a polycatenane thus obtained from **abc**. There are many possibilities, so with one exception, we limit ourselves to regular structures. Geometrical data are in Table 9.

Linked triangles. The only regular structure formed from a 4-c net is **lcy-y** (Fig. 41). However, there is at least one other with transitivity 1 1 1. This is obtained by taking the regular finite polycatenane formed from four triangles (12^4, Fig. 6). The twelve vertices can be linked as in face-centered cubic to produce the polycatenane with symbol **lkv** (Fig. 41). However, we do not consider it as a new regular polycatenane as it may also be considered as four interwoven **lcy-y** polycatenanes.

Linked quadrangles. We find two regular structures **sod-y** and **ana-y** (Fig. 42). Note that although the quadrangles in **ana-y** are not planar they are regular with equal (symmetry-related) edges and angles.

Table 9 Geometric data for 3-periodic polycatenanes. In the 'stick' column, that vertex is linked to the one in the 'corner' column. All have transitivity 1 1 1 except **lka** (2 1 1)

Symbol	Symmetry	Corner	Stick
lcv-y	$I4_132$	0.44, 0.19, 7/8	0.81, 3/8, 1.06
lkv	$F432$	0.3, 0, 0.7	0, 0.3, 1.3
sod-y	$Im\bar{3}m$	0.19, 0, 1/2	1/2, 0, 0.19
ana-y	$Ia\bar{3}d$	0.89, 0.42, 0.81	0.83, 0.14, 0.94
lka	$Fm\bar{3}c$	1/2, 0.2, 0	0.35, 1/2, 0
sod-y*	$Pn\bar{3}m$	0.31, 1/2, 0.69	0, 0.19, 0.69
ana-y*	$Ia\bar{3}d$	0.17, 0.30, 0.89	0.20, 0.39, 1.17
pcu-y	$Pm\bar{3}n$	0.1, 0.4, 3/4	0.9, 0.4, 3/4

This journal is © The Royal Society of Chemistry 2018

Published on 04 May 2018. Downloaded by University of California - Berkeley on 6/22/2018 6:56:28 PM.

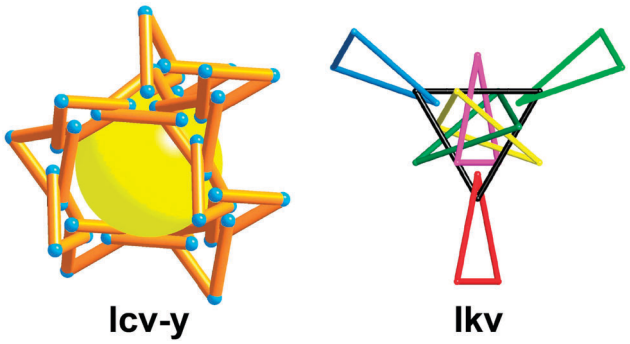

Fig. 41 Left: The polycatenane **lcv-y**. Linked triangles derived from the 4-c net **lcv**. Right: A fragment of a structure with transitivity 1 1 1 with each triangle linked to six others as shown for the black triangle. This structure is four interpenetrating **lcv-y** polycatenanes.

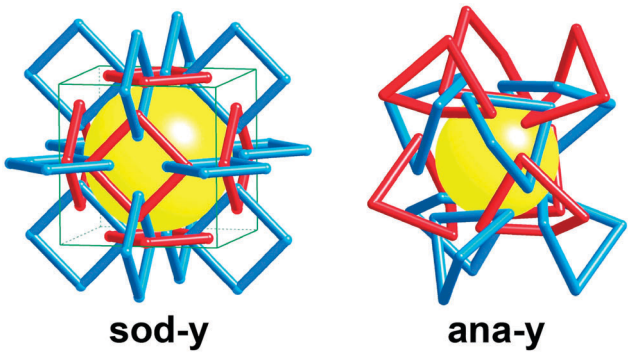

Fig. 42 Regular polycatenanes of linked quadrangles.

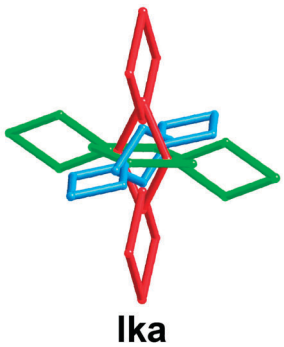

Fig. 43 A polycatenane with transitivity 2 1 1 formed by linking Borromean rings into a cubic framework.

We also show **lka** (Fig. 43), which is less regular (transitivity 2 1 1). This is made by linking Borromean sets of three rings (Fig. 4) into a cubic network. The structure can be considered to be interpenetrating 1-periodic chains with the Borromean property that no two chains are directly linked.

Linked hexagons. There are three regular structures (Fig. 44) **sod-y***, **ana-y***, and **lcs-y**. The skew ('chair') hexagons in **ana-y*** and **lcs-y** are regular (all edges and all angles related by symmetry).

Linked quadrangles with triple crossings. We have found one regular polycatenane derived from a 6-c net. This is **pcu-y** (Fig. 45) in which each quadrangle is linked to 8 others.

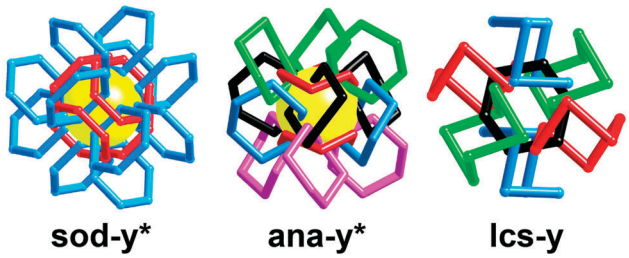

Fig. 44 Three regular polycatenanes formed by linking hexagons into a 3-periodic framework.

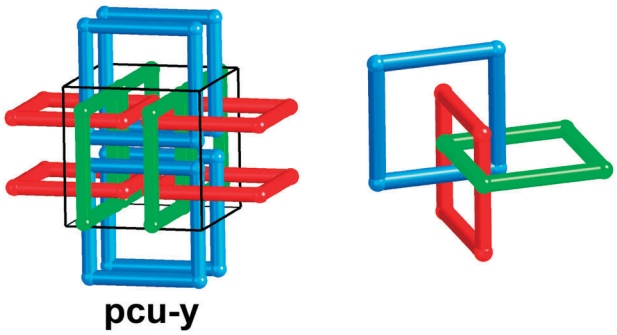

Fig. 45 A regular polycatenane constructed by interlocking quadrangles in a 6-c net.

4.5 Linked polyhedral

These structures (Fig. 46) are beyond our restriction to those made up solely of 2-c corners and sticks. However, one might argue that they are the true 3-periodic analogs of chainmail.

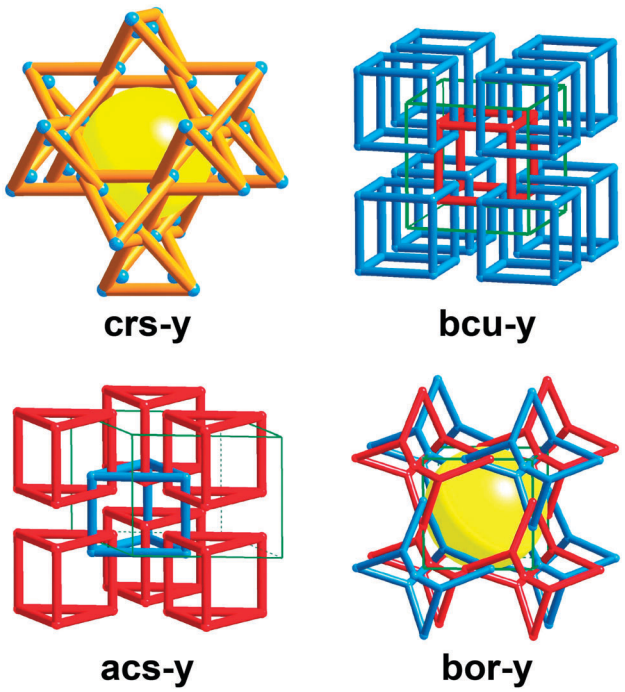

Fig. 46 Simple examples of 3-periodic 'chainmail' formed by linking polyhedra into 3-periodic frameworks.

Published on 04 May 2018. Downloaded by University of California - Berkeley on 6/22/2018 6:56:28 PM.

crs-y (linked tetrahedra) and **bcu-y** (linked cubes) are the only ones with one kind of edge and one kind of vertex. **acs-y** has two kinds of stick (edge). **bor-y** is derived from the boracite net (**bor**) and can be considered as linked adamantane units with 2-c and 3-c vertices. We include it as it forms the basis for a rare example of a crystal structure based on 3-periodic chainmail.[73]

4.6 Mixed threads and rings

We show here some examples of structures with interwoven threads and rings (Fig. 47). They all have the minimal possible transitivity (2 2 2) and, as in earlier examples of dinemal weavings, one kind of link point. Symbols are **abc-wy** for structures derived from **abc**.

In addition, **unw-wy** is formed from triangles and 3_1 (or 3_2) helices. The helix axes are in the Ω rod packing as in **sod-w** but now linked with triangles as shown in the figure. Finally, **unx-wy** has again triangles in four orientations (parallel to ⟨111⟩) but now the threads are 4_1 (or 4_3) helices. The structure is hard to illustrate but can be appreciated by the observation that the yellow ball in the figure is part of a **dia** (diamond) array of such balls (Table 10).

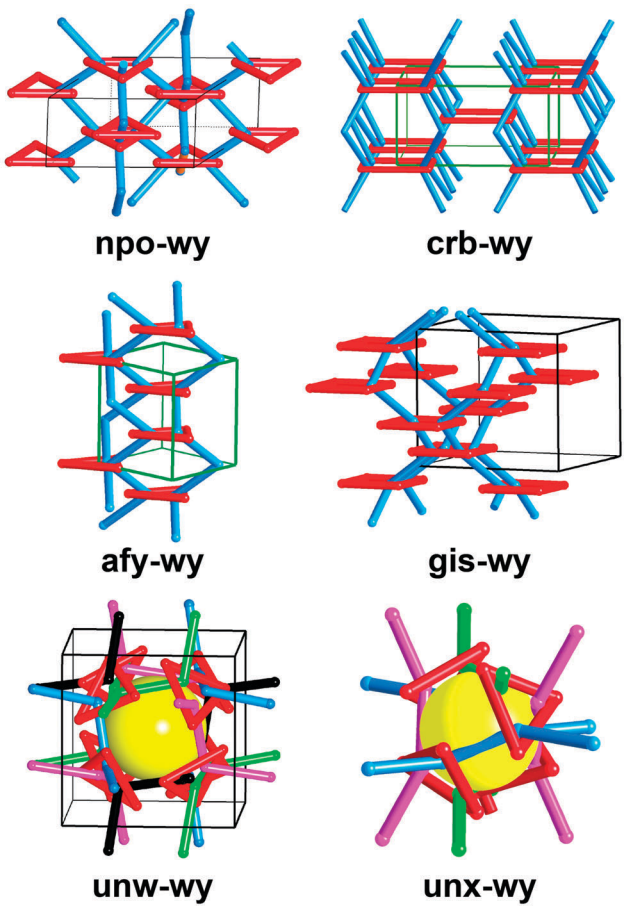

Fig. 47 Examples of interwoven combinations of threads and rings with transitivity 2 2 2. Those with parallel threads and parallel rings are: **npo-wy** triangles and zigzags; **crb-wy** squares and zigzags; **afw-wy** triangles and 3_1 (or 3_2) helices; **gis-wy** squares and 4_1 and 4_3 helices.

Table 10 Geometric data for 3-periodic thread plus ring weavings with transitivity 2 2 2. The vertex in the 'stick' column is linked to the one in the 'corner' column

Symbol	Symmetry	Corner	Stick
npo-wy	$P6_5/mmc$	0.47, 0.53, 1/4	0, 0.53, 1/4
		0.41, 0.82, 1/4	0.59, 1.18, 3/4
crb-wy	$I4/mmm$	0.72, 0.28, 1/2	0.72, 0.72, 1/2
		0.17, 0.17, 0	0.33, 0.33, 1/2
afw-wy	$R32$	0.125, 0, 0	0.542, 0.208, 1/3
		1/3, 0.6, 1/3	0.4, 0.067, 1/3
gis-wy	$I4_1/amd$	0.1, 0.35, 7/8	0.4, 0.35, 5/8
		0.1, 0.45, 7/8	0.2, 0.05, 7/8
unw-wy	$I432$	1/4, 0.19, 0.31	0.19, 1/4, 0.61
		1/4, 0.08, 0.42	0.08, 0.42, 1/4
unx-wy	$I4_132$	0.125, 0, 1/4	1/4, 0.125, 0
		1/8, 0.06, 0.19	3/8, 0.06, 0.31

5. Realization of synthetic targets – present and future

5.1 Synthetic strategy and design of polycatenated and woven structures by using metal complexes as templates

The designed synthesis of 0-periodic molecular knots and catenanes is well documented in the chemical literature.[39–48,50,52,74] The first proof-of-concept work in the field was reported in 1960 with the successful synthesis of a [2]catenane by statistical interlocking of molecular macrocycles.[75] In 1964, the first directed synthesis of a catenane was demonstrated by introducing a covalent template to put the two molecular components in place.[76] Upon subsequent cleavage of this covalent template the catenated molecule was obtained in higher yields as compared to the previously reported statistical approach However, the synthesis still required many steps and thus the overall yield was still low. The breakthrough for the field took place in 1983 when a metal-template approach was disclosed to construct higher-order molecular architectures.[77] This strategy has several advantages with regard to the designed synthesis of catenated architectures: (1) high overall yield, (2) simple building blocks (can be simply functionalized ligands), and (3) specific orientation of the ligands as a result of metal coordination to the template allowing for efficient formation of the entanglement. The ability of synthetic chemists to construct increasingly complex molecular structures has since then progressed remarkably and a plethora of highly sophisticated 0-periodic structures has been achieved as reviewed in Sections 1 and 2.

On a conceptual level, we view the synthesis of extended 2- and 3-periodic polycatenanes and weaving structures as an extension to their discrete molecular counterparts. We believe that a similar template strategy in conjunction with the design principles of Reticular Synthesis, which describes the reticulation of molecular building blocks to construct extended crystalline frameworks, can be employed to target such polycatenated and woven structures. Here again we start from a molecular metal complex with functionalized organic ligands, but instead of forming discrete molecules by non-propagating ring closing reactions, they are linked to form 2- and 3-periodic framework structures through the formation of strong, directional bonds. The directionality of the bonds is crucial as, in conjunction with the adjustment of angles and metrics of the molecular

 This journal is © The Royal Society of Chemistry 2018

Published on 04 May 2018. Downloaded by University of California - Berkeley on 6/22/2018 6:56:28 PM.

constituents, it allows for the resulting woven structures to be designed with regard to their underlying weaving.

A first example of a woven extended structure was reported as COF-505,[71] a covalent organic **dia-w** framework (COF). Analogous to the aforementioned synthesis of the first molecular catenane, its synthesis relies on a copper(I)-bisphenanthroline complex as the template. Instead of a terminating ring closing reaction in the molecular structure, the complex is reticulated into an extended framework structure of **dia** net through reversible imine bond formation using benzidine as a linker (Scheme 1). In both scenarios the metal template needs to be removed post-synthetically to yield the 0-periodic Hopf link [2]catenane and 3-periodic woven **dia-w** structure, respectively.

The same design strategy for constructing woven structures can be applied to other metal complexes that are stable under the solvothermal conditions used in COF synthesis. Another woven framework, COF-112, has also been successfully synthesized (Scheme 2) by linking the amine-functionalized cobalt bis(diiminopyridine) complex, [Co(NH_2-DIP)$_2$]. The tetrahedral complex has a dihedral angle (between the two pyridine rings) of 80°, close to the angle of 90° of a **dia** net in its highest symmetry embedding. In addition, *tert*-butyloxycarbonyl (Boc) groups were utilized to protect the primary amines in the starting materials. This increases the solubility of the starting reagents as well as intermediates, allowing for the maximum degree of error correction of the intermediates during the dynamic bond formation. This procedure yields a well-defined extended COF framework that consists of interlacing 1D zigzag polyimine chains.

5.2 Future prospects

It is no coincidence that the first examples of woven COFs features a **dia-w** weaving. The synthetic route toward the structure relies on the initial formation of a **dia** framework, which is only subsequently demetalated to yield the derived woven framework. Since the diamond net is the default structure for tetrahedral nets it is the most likely to form in the context of reticular synthesis. The advantage of using COFs to target woven or polycatenated extended structures is however that the directional covalent bonds and the rigid organic building blocks allow for the adjustment of angles and therefore for targeting of topologies other than the default nets. As such, these angles must not be understood as a strict necessity for the formation of the desired topologies but more as a guideline for their design. In a regular weaving or polycatenane, the nature of the thread or ring depends on the geometry of three contiguous sticks expressed as the corner angle between neighboring sticks and the dihedral angle between next-neighbor sticks. For example, if the corner angle is the tetrahedral angle, 109.5°, the following geometries result for different dihedral angles: 30°, skew

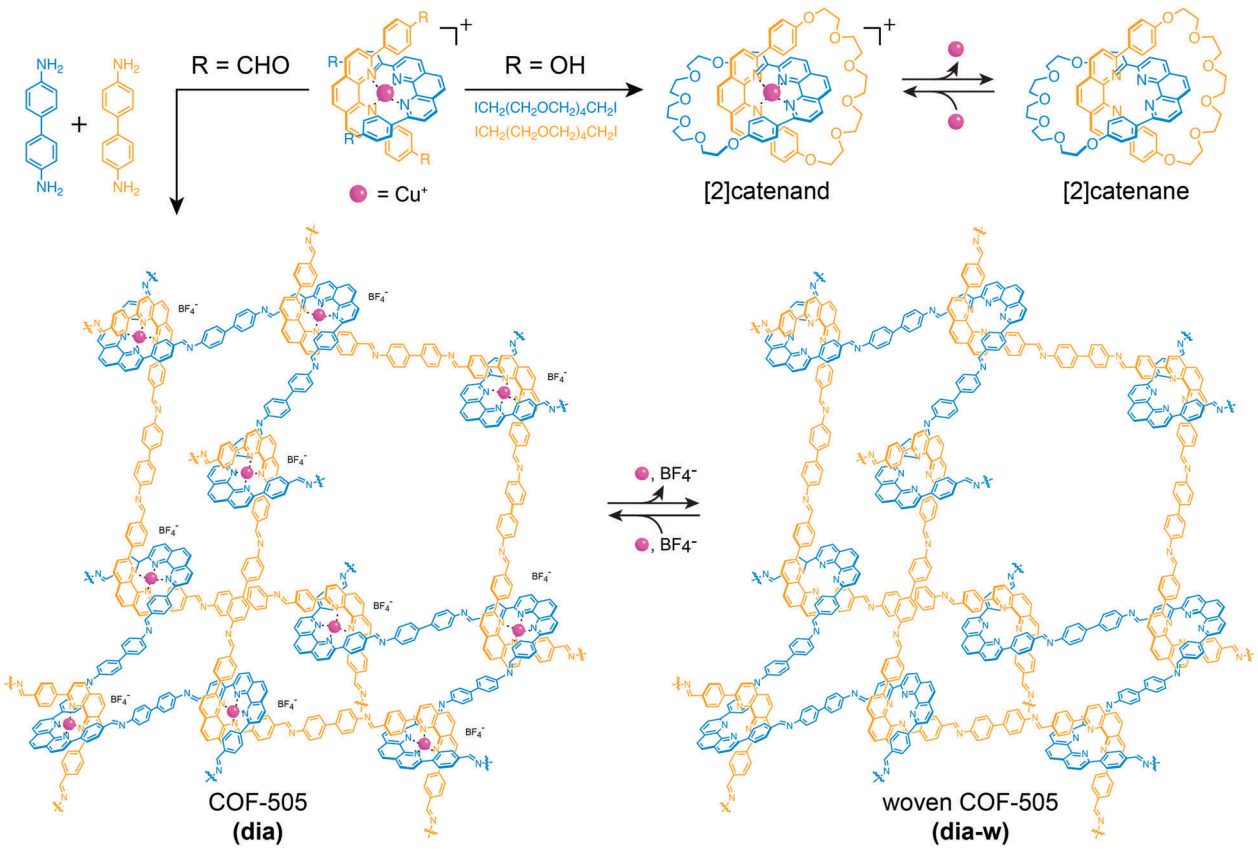

Scheme 1 Synthetic routes for molecular [2]catenane and extended woven COF-505 by employing the copper(I)-bisphenanthroline core as a template. Threads in blue and orange are chemically identical; colors are used to highlight the threads with different propagation directions.

Published on 04 May 2018. Downloaded by University of California - Berkeley on 6/22/2018 6:56:28 PM.

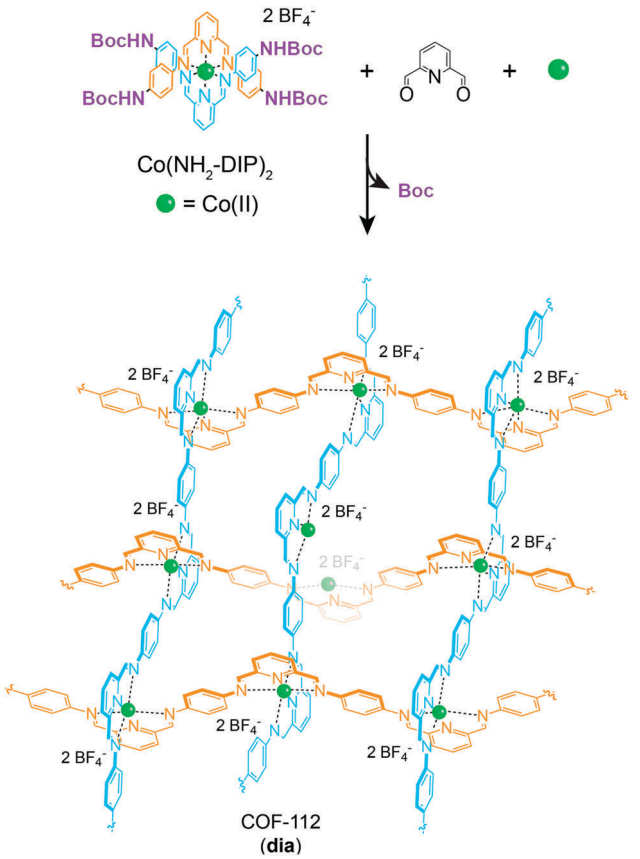

Scheme 2 Synthetic route for the crystalline woven COF-112 by employing Co(II) ions as a template.

('chair') hexagon; 60° tetragonal helix; 109.5°, trigonal helix, 180°, zigzag; a hexagonal helix is not possible.

In Table 11 we have compiled a concise list of regular woven and polycatenated nets with optimal girth greater than 0.25. We also give the corner angle (ϕ) and crossing angle (ψ) derived from their optimal embeddings. The crossing angle, with one exception, is 90° for double crossings. Structures with triple crossings should be accessible using a templating complex with 32 (D_3) symmetry. **pcu-w** and **crs-w** with zigzag threads should be prime targets. We expect that the list, alongside the general design considerations outlined above, will serve as a guideline for the targeted synthesis of a large variety of woven and polycatenated frameworks of different structure types. Equally important is the fact that knowing a small group of expected structures can be of crucial help in both predicting and determining the crystal structures.[78]

Finally, we remark that we make no claim to completeness in our identification of regular structures. We have noted that, for example, **pcu-w**, **sod-w**, and **pcu-w*** all have vertices in the same Wyckoff set (24 g of *I*432) but with sticks defined by different pairs of vertices. It is likely that other regular structures, but with smaller girth, could be found from other combinations. But we do feel that we have discovered the majority of the high-girth weavings that are of most interest in chemistry.

Table 11 The weavings with largest girth at optimal embedding. Under 'type', F indicates fabric weave and C indicates chain-link weave; the following numbers indicate a double (2) or triple (3) link

Symbol	Girth	Thread	Type	ϕ [°]	ψ [°]
nbo-w	0.619	4_1 and 4_3	F2	139.0	90
qtz-w**	0.450	6_1 or 6_5	C2	129.6	73.8
lcs-w	0.429	4_1 and 4_3	C2	108.2	90
dia-w*	0.408	4_1 or 4_3	C2	109.5	90
acs-w	0.315	6_1 or 6_5	C3	135.6	—
qtz-w*	0.310	3_1 or 3_2	C2	78.5	90
dia-w	0.294	2_1	C2	95.4	90
crs-w	0.277	2_1	F3	113.0	—
pcu-w	0.253	2_1	F3	94.6	—
lcy-w	0.252	3_1 or 3_2	C3	108.3	—

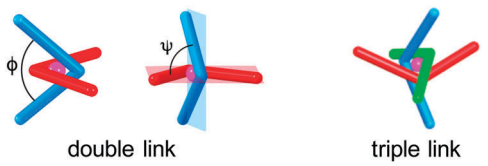

Conflicts of interest

There are no conflicts to declare.

Acknowledgements

Y. L. acknowledges funding from the Philomathia Graduate Fellowship in the Environmental Sciences.

References

1 Knot Atlas, http://katlas.org/wiki/Main_Page.
2 C. C. Adams, *The Knot Book*, American Mathematical Soc., 1994.
3 H. W. Gibson, M. C. Bheda and P. T. Engen, *Prog. Polym. Sci.*, 1994, **19**, 843–945.
4 Z. Niu and H. W. Gibson, *Chem. Rev.*, 2009, **109**, 6024–6046.
5 C. J. Bruns and J. F. Stoddart, *The nature of the mechanical bond: from molecules to machines*, John Wiley & Sons, 2016.
6 C. O. Dietrich-Buchecker and J.-P. Sauvage, *Chem. Rev.*, 1987, **87**, 795–810.
7 R. S. Forgan, J. P. Sauvage and J. F. Stoddart, *Chem. Rev.*, 2011, **111**, 5434–5464.
8 G. Gil-Ramírez, D. A. Leigh and A. J. Stephens, *Angew. Chem., Int. Ed.*, 2015, **54**, 6110–6150.
9 O. M. Yaghi, M. O'Keeffe, N. W. Ockwig, H. K. Chae, M. Eddaoudi and J. Kim, *Nature*, 2003, **423**, 705–714.
10 H. Furukawa, K. E. Cordova, M. O'Keeffe and O. M. Yaghi, *Science*, 2010, **9**, 1230444.
11 C. S. Diercks and O. M. Yaghi, *Science*, 2017, **355**, eaal1585.
12 M. O'Keeffe, *Acta Crystallogr., Sect. A: Found. Crystallogr.*, 2008, **64**, 425–429.
13 M. O'Keeffe, M. A. Peskov, S. J. Ramsden and O. M. Yaghi, *Acc. Chem. Res.*, 2008, **41**, 1782–1789.
14 M. Li, D. Li, M. O'Keeffe and O. M. Yaghi, *Chem. Rev.*, 2014, **114**, 1343–1370.

This journal is © The Royal Society of Chemistry 2018

Published on 04 May 2018. Downloaded by University of California - Berkeley on 6/22/2018 6:56:28 PM.

15 O. Delgado Friedrichs, M. O'Keeffe and O. M. Yaghi, *Acta Crystallogr., Sect. A: Found. Crystallogr.*, 2003, **59**, 22–27.
16 O. Delgado-Friedrichs and M. O'Keeffe, *Acta Crystallogr., Sect. A: Found. Crystallogr.*, 2003, **59**, 351–360.
17 V. Kopský and D. B. Litvin, *International Tables for Crystallography, Volume E: Subperiodic Groups*, International Union of Crystallography, Chester, England, 2006, vol. E.
18 B. Grunbaum and G. C. Shephard, *Am. Math. Mon.*, 1988, **95**, 5–30.
19 S. R. Batten and R. Robson, *Angew. Chem., Int. Ed.*, 1998, **37**, 1460–1494.
20 E. V. Alexandrov, V. A. Blatov and D. M. Proserpio, *Acta Crystallogr., Sect. A: Found. Crystallogr.*, 2012, **68**, 484–493.
21 S. T. Hyde, B. Chen and M. O'Keeffe, *CrystEngComm*, 2016, **18**, 7607–7613.
22 L. Carlucci, G. Ciani and D. M. Proserpio, *Coord. Chem. Rev.*, 2003, **246**, 247–289.
23 V. A. Blatov, L. Carlucci, G. Ciani and D. M. Proserpio, *CrystEngComm*, 2004, **6**, 377–395.
24 C. Bonneau and M. O'Keeffe, *Acta Crystallogr., Sect. A: Found. Crystallogr.*, 2015, **71**, 82–91.
25 I. A. Baburin, *Acta Crystallogr., Sect. A: Found. Adv.*, 2016, **72**, 366–375.
26 R. A. Bissell, E. Córdova, A. E. Kaifer and J. F. Stoddart, *Nature*, 1994, **369**, 133–137.
27 B. F. Hoskins, R. Robson and D. A. Slizys, *J. Am. Chem. Soc.*, 1997, **119**, 2952–2953.
28 N. Armaroli, V. Balzani, J. P. Collin, P. Gaviña, J. P. Sauvage and B. Ventura, *J. Am. Chem. Soc.*, 1999, **121**, 4397–4408.
29 S. A. Nepogodiev and J. F. Stoddart, *Chem. Rev.*, 1998, **98**, 1959–1976.
30 T. Takata, *Polym. J.*, 2006, **38**, 1–20.
31 A. Coskun, M. Hmadeh, G. Barin, F. Gándara, Q. Li, E. Choi, N. L. Strutt, D. B. Cordes, A. M. Z. Slawin, J. F. Stoddart, J. P. Sauvage and O. M. Yaghi, *Angew. Chem., Int. Ed.*, 2012, **51**, 2160–2163.
32 H. Deng, M. A. Olson, J. F. Stoddart and O. M. Yaghi, *Nat. Chem.*, 2010, **2**, 439–443.
33 K. Zhu, C. a O'Keefe, V. N. Vukotic, R. W. Schurko and S. J. Loeb, *Nat. Chem.*, 2015, **7**, 514–519.
34 P. R. McGonigal, P. Deria, I. Hod, P. Z. Moghadam, A.-J. Avestro, N. E. Horwitz, I. C. Gibbs-Hall, A. K. Blackburn, D. Chen, Y. Y. Botros, M. R. Wasielewski, R. Q. Snurr, J. T. Hupp, O. K. Farha and J. F. Stoddart, *Proc. Natl. Acad. Sci. U. S. A.*, 2015, **112**, 11161–11168.
35 V. Nicholas Vukotic, C. A. O'Keefe, K. Zhu, K. J. Harris, C. To, R. W. Schurko and S. J. Loeb, *J. Am. Chem. Soc.*, 2015, **137**, 9643–9651.
36 P. J. Paukstelis and N. C. Seeman, *Crystals*, 2016, **6**, 97.
37 M. R. Jones, N. C. Seeman and C. A. Mirkin, *Science*, 2015, **347**, 1260901.
38 F. Hong, F. Zhang, Y. Liu and H. Yan, *Chem. Rev.*, 2017, **117**, 12584–12640.
39 C. O. Dietrich-Buchecker and J.-P. Sauvage, *Angew. Chem., Int. Ed. Engl.*, 1989, **28**, 189–192.
40 J.-F. Ayme, J. E. Beves, D. A. Leigh, R. T. McBurney, K. Rissanen and D. Schultz, *Nat. Chem.*, 2011, **4**, 15–20.
41 S. D. P. Fielden, D. A. Leigh and S. L. Woltering, *Angew. Chem., Int. Ed.*, 2017, **56**, 11166–11194.
42 J. J. Danon, A. Krüger, D. A. Leigh, J. Lemonnier, A. J. Stephens, I. J. Vitorica-yrezabal and S. L. Woltering, *Science*, 2017, **162**, 159–162.
43 N. Ponnuswamy, F. B. L. Cougnon, G. D. Pantoş and J. K. M. Sanders, *J. Am. Chem. Soc.*, 2014, **136**, 8243–8251.
44 C. Dietrich-Buchecker and J.-P. Sauvage, *J. Am. Chem. Soc.*, 1984, **106**, 3043–3045.
45 J. F. Nierengarten, C. O. Dietrich-Buchecker and J. P. Sauvage, *J. Am. Chem. Soc.*, 1994, **116**, 375–376.
46 J.-P. Sauvage, *Acc. Chem. Res.*, 1998, **31**, 611–619.
47 S. M. Goldup, D. A. Leigh, T. Long, P. R. McGonigal, M. D. Symes and J. Wu, *J. Am. Chem. Soc.*, 2009, **131**, 15924–15929.
48 D. A. Leigh, R. G. Pritchard and A. J. Stephens, *Nat. Chem.*, 2014, **6**, 978–982.
49 C. Lincheneau, B. Jean-Denis and T. Gunnlaugsson, *Chem. Commun.*, 2014, **50**, 2857.
50 C. S. Wood, T. K. Ronson, A. M. Belenguer, J. J. Holstein and J. R. Nitschke, *Nat. Chem.*, 2015, **7**, 354–358.
51 Q. Wu, P. M. Rauscher, X. Lang, R. J. Wojtecki, J. J. de Pablo, M. J. A. Hore and S. J. Rowan, *Science*, 2017, **358**, 1434–1439.
52 K. S. Chichak, S. J. Cantrill, A. R. Pease, S.-H. Chiu, G. W. V. Cave, J. L. Atwood and J. F. Stoddart, *Science*, 2004, **304**, 1308–1312.
53 G.-P. Yang, L. Hou, X.-J. Luan, B. Wu and Y.-Y. Wang, *Chem. Soc. Rev.*, 2012, **41**, 6992–7000.
54 L. Han and Y. Zhou, *Inorg. Chem. Commun.*, 2007, **11**, 385–387.
55 A. M. Champsaur, C. Mézière, M. Allain, D. W. Paley, M. L. Steigerwald, C. Nuckolls and P. Batail, *J. Am. Chem. Soc.*, 2017, **139**, 11718–11721.
56 Z. Wang, A. Błaszczyk, O. Fuhr, S. Heissler, C. Wöll and M. Mayor, *Nat. Commun.*, 2017, **8**, 14442.
57 P. M. Van Calcar, M. M. Olmstead and A. L. Balch, *J. Chem. Soc., Chem. Commun.*, 1995, 1773–1774.
58 Y.-H. Li, C.-Y. Su, A. M. Goforth, K. D. Shimizu, K. D. Gray, M. D. Smith and H.-C. zur Loye, *Chem. Commun.*, 2003, 1630–1631.
59 U. Lewandowska, W. Zajaczkowski, S. Corra, J. Tanabe, R. Borrmann, E. M. Benetti, S. Stappert, K. Watanabe, N. A. K. Ochs, R. Schaeublin, C. Li, E. Yashima, W. Pisula, K. Müllen and H. Wennemers, *Nat. Chem.*, 2017, **9**, 1068–1072.
60 S. LaPlantz, *The Mad Weave Book an Ancient Form of Triaxial Basket Weaving*, Dover Publications, 2016.
61 P. Gailiunas, *J. Math. Arts*, 2017, **11**, 40–58.
62 J.-P. Zhang, X.-L. Qi, C.-T. He, Y. Wang and X.-M. Chen, *Chem. Commun.*, 2011, **47**, 4156–4158.
63 F. L. Thorp-Greenwood, A. N. Kulak and M. J. Hardie, *Nat. Chem.*, 2015, **7**, 526–531.
64 M. E. Evans, V. Robins and S. T. Hyde, *Acta Crystallogr., Sect. A: Found. Crystallogr.*, 2013, **69**, 262–275.
65 E. V. Alexandrov, A. V. Goltsev, M. O'Keeffe and D. M. Proserpio, *Cryst. Growth Des.*, 2017, **17**, 2941–2944.

Published on 04 May 2018. Downloaded by University of California - Berkeley on 6/22/2018 6:56:28 PM.

66 N. L. Rosi, J. Kim, M. Eddaoudi, B. Chen, M. O. Keeffe and O. M. Yaghi, *J. Am. Chem. Soc.*, 2005, **127**, 1504–1518.
67 T. Verhoeff and K. Verhoeff, *Proceedings of Bridges 2011: Mathematics, Music, Art, Architecture, Culture (14th Annual Conference, Coimbra, Portugal, July 2011)*, Tessellations Publishing, 2011, pp. 1–8.
68 A. Stasiak, V. Katritch and L. H. Kauffman, *Ideal Knots*, World Scientific, 1998, vol. 19.
69 M. E. Evans, V. Robins and S. T. Hyde, *Proc. R. Soc. A*, 2015, **471**, 20150254.
70 M. Li, C. R. Ye, X. C. Huang and M. O'Keeffe, *Struct. Chem.*, 2017, **28**, 147–152.
71 Y. Liu, Y. Ma, Y. Zhao, X. Sun, F. Gandara, H. Furukawa, Z. Liu, H. Zhu, C. Zhu, K. Suenaga, P. Oleynikov, A. S. Alshammari, X. Zhang, O. Terasaki and O. M. Yaghi, *Science*, 2016, **351**, 365–369.
72 Y. Zhao, L. Guo, F. Gándara, Y. Ma, Z. Liu, C. Zhu, H. Lyu, C. A. Trickett, E. A. Kapustin, O. Terasaki and O. M. Yaghi, *J. Am. Chem. Soc.*, 2017, **139**, 13166–13172.
73 X. F. Kuang, X. Y. Wu, R. M. Yu, J. P. Donahue, J. S. Huang and C. Z. Lu, *Nat. Chem.*, 2010, **2**, 461–465.
74 J. E. Beves, J. J. Danon, D. A. Leigh, J. F. Lemonnier and I. J. Vitorica-Yrezabal, *Angew. Chem., Int. Ed.*, 2015, **54**, 7555–7559.
75 E. Wassermann, *J. Am. Chem. Soc.*, 1960, **82**, 4433–4434.
76 G. Schill and A. Lüttringhaus, *Angew. Chem., Int. Ed. Engl.*, 1964, **3**, 546–547.
77 C. O. Dietrich-Buchecker, J. P. Sauvage and J. P. Kintzinger, *Tetrahedron Lett.*, 1983, **24**, 5095–5098.
78 H. M. El-Kaderi, J. R. Hunt, J. L. Mendoza-Cortés, A. P. Côté, R. E. Taylor, M. O'Keeffe and O. M. Yaghi, *Science*, 2007, **316**, 268–272.

 This journal is © The Royal Society of Chemistry 2018